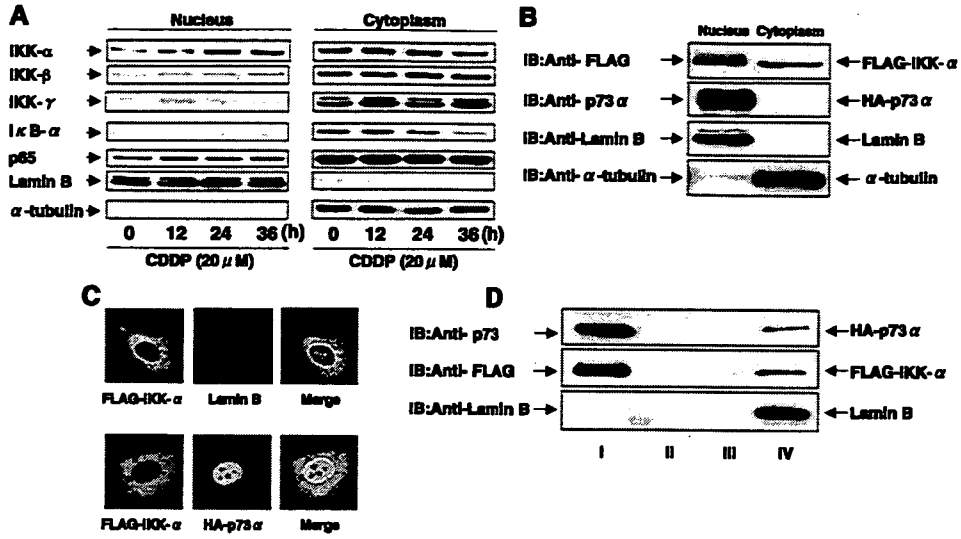

FIGURE 2. **Nuclear accumulation of IKK-α.** *A*, nuclear accumulation of IKK-α in response to CDDP. At the indicated time periods after the addition of CDDP, U2OS cells were fractionated into nuclear and cytoplasmic fractions and then analyzed by immunoblotting with the indicated antibodies. Anti-lamin B and anti-α-tubulin immunoblotting were included to assess the purity of each fraction. *B*, subcellular localization of exogenous IKK-α. U2OS cells were transiently transfected with the expression plasmid for FLAG-IKK-α or HA-p73α. Cells were subjected to biochemical fractionation, followed by immunoblotting (*IB*) with anti-FLAG or anti-p73 antibody. *C*, co-localization of IKK-α and p73 in nuclear laminae. U2OS cells were transiently transfected with the FLAG-IKK-α expression plasmid alone (*upper panels*) or with the HA-p73α expression plasmid (*lower panels*). Cells were processed for indirect immunofluorescence and double-stained with anti-FLAG and anti-lamin B antibodies (*upper panels*) or with anti-HA and anti-FLAG antibodies (*lower panels*). The merged images show that IKK-α co-localized with p73α in nuclear laminae (*yellow*). *D*, p73α and IKK-α are detected in the nuclear matrix fraction. U2OS cells cotransfected with the expression plasmids for HA-p73α and FLAG-IKK-α were subjected to high salt nuclear matrix fractionation as described under "Experimental Procedures." Each fraction was analyzed by immunoblotting with anti-p73 (*upper panel*), anti-IKK-α (*middle panel*), or anti-lamin B (*lower panel*) antibody.

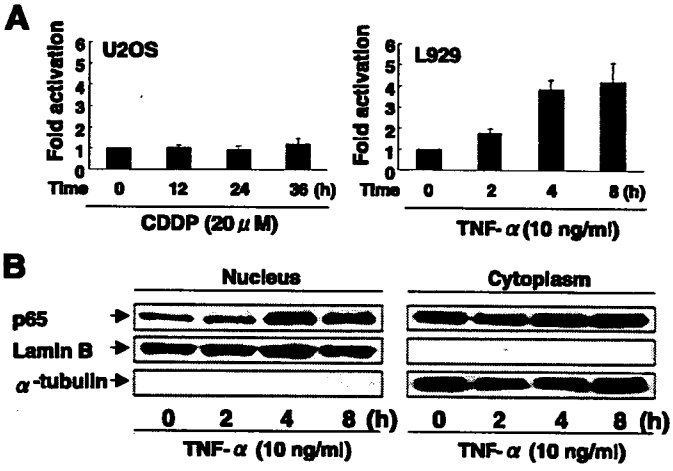

FIGURE 3. **NF-κB is not activated in response to CDDP.** *A*, U2OS (*left panel*) or L929 (*right panel*) cells were cotransfected with the NF-κB reporter construct (pELAM1-Luc) and the *Renilla* luciferase plasmid (pRL-tk). Twenty-four hours after transfection, U2OS and L929 cells were treated with CDDP and TNF-α, respectively. At the indicated time points after treatment, luciferase activity was determined. *B*, nuclear accumulation of p65 in L929 cells exposed to TNF-α. At the indicated time periods after treatment with TNF-α, L929 cells were fractionated into nuclear and cytoplasmic fractions and then analyzed directly by immunoblotting with anti-p65 antibody.

the cytoplasm and nuclear lamina, as indicated by the extensive co-localization with lamin B, a nuclear lamina marker (Fig. 2*C*). Intriguingly, HA-p73α was co-localized with FLAG-IKK-α in the nuclear lamina of the transfected cells. To confirm these observations, nuclear matrix fractionation was performed 48 h after transfection, and the fractions obtained were subjected to immunoblotting. As shown in Fig. 2*D*, HA-p73α and FLAG-IKK-α were detected in nuclear matrix fraction (fraction IV). Our results suggest that nuclear IKK-α might interact with pro-apoptotic p73α and modulate its function.

As described above, the amounts of the nuclear transactivating p65 subunit remained unchanged in U2OS cells treated with CDDP. These findings prompted us to examine whether NF-κB activation can be detected in response to CDDP. To this end, U2OS cells transfected with the NF-κB reporter plasmid (40) were treated with CDDP, and their luciferase activity was determined. Consistent with the previous observations (13), CDDP treatment did not enhance NF-κB-dependent transcriptional activation (Fig. 3*A*, *left panel*). Under our experimental conditions, NF-κB-dependent transcriptional activation was detected within 2 h of exposure to TNF-α in the mouse fibrosarcoma cell line L929 (Fig. 3*A*, *right panel*), which is widely used to investigate TNF-α-dependent NF-κB activation (41). In addition, treatment of L929 cells with TNF-α caused a nuclear accumulation of p65 (Fig. 3*B*). Thus, it is likely that, the lack of a significant effect of CDDP on NF-κB-dependent transcriptional activation could be attributed to lack of the regulated nuclear accumulation of p65.

IKK-α Interacts with p73—To determine whether IKK-α can interact with p73 in cells, whole cell lysates prepared from transfected COS-7 cells were immunoprecipitated with anti-FLAG or anti-HA antibody and analyzed by immunoblotting using anti-p73 or anti-FLAG antibody, respectively. As shown in Fig. 4*A*, exogenously expressed FLAG-IKK-α and HA-p73α formed stable complexes in COS-7 cells. Similarly, HA-p73β was co-immunoprecipitated with FLAG-IKK-α (data not shown). Their interaction was further examined using endogenous materials. As shown in Fig. 4*B*, endogenous p73α formed a protein complex with endogenous IKK-α in U2OS cells exposed to CDDP. Similar results were also obtained in HeLa cells (data not shown). In contrast, immunoprecipitation of endogenous p53 followed by immunoblotting with anti-FLAG antibody did not detect co-immunoprecipitated FLAG-IKK-α (Fig. 4*C*), indicating that IKK-α interacts with p73, but not with p53, in cells. To identify the p73 determinants involved in the interaction with IKK-α, we generated several deletion mutants of p73α fused to GST and tested their ability to bind to FLAG-IKK-α in GST pulldown assays. These mutants were designed based on p73α, including the transactivation, DNA-binding,

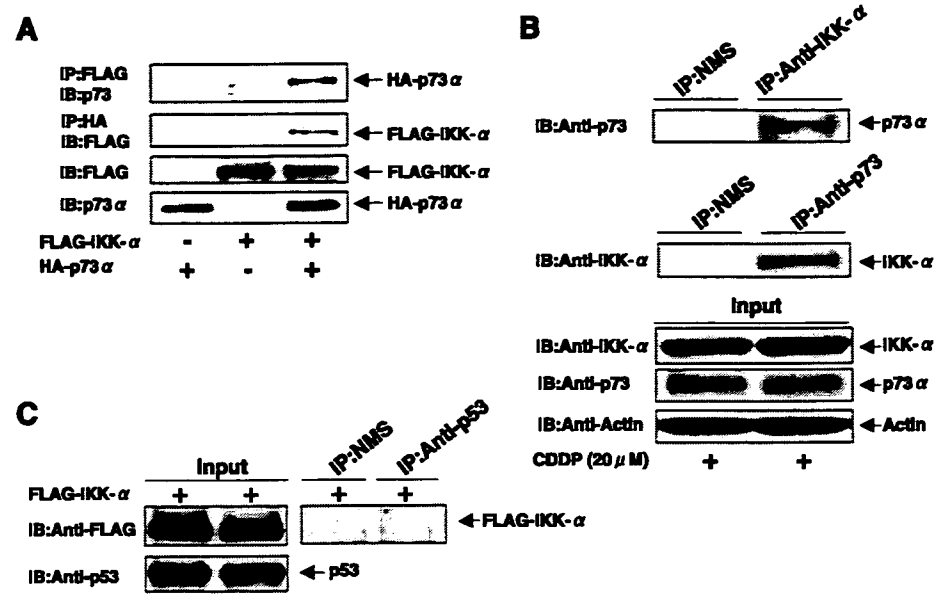

FIGURE 4. **Interaction between IKK-α and p73α.** *A*, FLAG-IKK-α was transiently coexpressed with HA-p73α in COS-7 cells as indicated. Whole cell lysates were subjected to immunoprecipitation (*IP*) with anti-FLAG or anti-HA antibody, followed by immunoblotting (*IB*) with anti-p73 or anti-FLAG antibody, respectively. *B*, whole cell lysates were prepared from U2OS cells exposed to CDDP and subjected to immunoprecipitation with normal mouse serum (*NMS*), anti-IKK-α antibody, or anti-p73 antibody, followed by immunoblotting with the indicated antibodies. *C*, FLAG-IKK-α was transiently transfected into COS-7 cells. Whole cell lysates were subjected to immunoprecipitation with normal mouse serum or anti-p53 antibody, followed by immunoblotting with anti-FLAG antibody. *Input* represents the 10% materials used for immunoprecipitation in *B* and *C*.

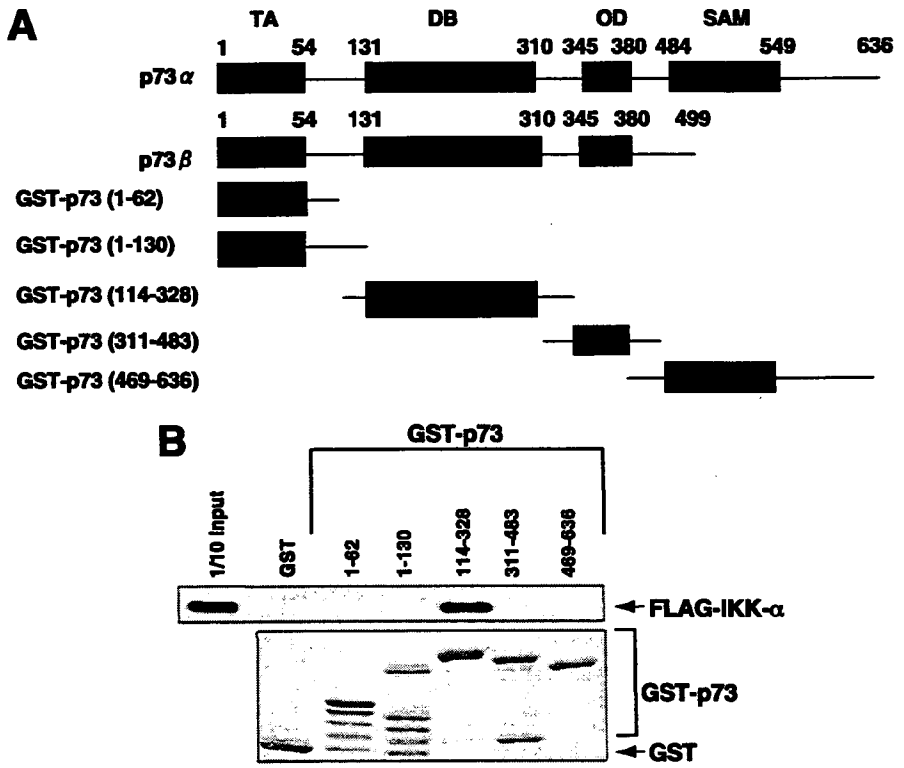

FIGURE 5. **DNA-binding domain of p73α is required for interaction with IKK-α.** *A*, shown is a schematic representation of the GST-p73 fusion proteins. *TA*, transactivation domain; *DB*, DNA-binding domain; *OD*, oligomerization domain; *SAM*, sterile α-motif domain. *B*, the DNA-binding domain of p73α is required for the interaction with IKK-α. ^{35}S-Labeled FLAG-IKK-α was incubated with GST or the indicated GST-p73 fusion proteins, and bound radiolabeled proteins were recovered on glutathione-Sepharose beads and visualized by autoradiography. The 1/10 volumes of input sample (*1/10 Input*) of ^{35}S-labeled FLAG-IKK-α used for pulldown assay were applied to the same gel (*upper panel*). Coomassie Blue-stained GST-p73 fusion proteins together with GST are also shown (*lower panel*).

oligomerization, and sterile α-motif domains (Fig. 5*A*). As shown in Fig. 5*B*, radiolabeled FLAG-IKK-α bound to GST-p73-(114–328), but not to the other GST fusion proteins. Taken together, our results suggest that IKK-α directly interacts with p73 through its DNA-binding domain.

IKK-α Increases p73 Stability—As described previously (16, 42), some p73-interacting protein kinases, including c-Abl and protein kinase Cδ, can stabilize p73. To investigate whether IKK-α can affect the stability of p73, COS-7 cells were transiently cotransfected with equal amounts of the HA-p73α expression plasmid with or without increasing amounts of the expression plasmid encoding IKK-α, and the protein level of HA-p73α was examined. As shown in Fig. 6*A*, the amount of HA-p73α was significantly increased in the presence of exogenous IKK-α, whereas IKK-α had no detectable impact on the stability of FLAG-p53. In addition, HA-p73β was also stabilized by IKK-α, but to a lesser degree compared with HA-p73α. *p73α* mRNA levels remained unchanged in the presence of IKK-α (Fig. 6*A*, *lower panels*), suggesting that IKK-α regulates p73 at the protein level. Next, we examined the possible effect of IKK-β on the stability of p73 and p53 by transient cotransfection. As shown in Fig. 6*B*, FLAG-IKK-β had negligible effects on the stability of both p73α and p53.

To investigate a possible role of endogenous IKK-α in the regulation of p73 stability, we employed RNA interference to block IKK-α expression. The enforced expression of siRNA against IKK-α in U2OS cells resulted in a significant reduction of endogenous IKK-α (Fig. 6*C*). We then tested the effect of knockdown of endogenous IKK-α on the CDDP-mediated accumulation of p73α. U2OS cells were transiently transfected with the expression plasmid for siRNA against IKK-α and exposed to CDDP for 36 h. As shown in Fig. 6*C*, down-regulation of endogenous IKK-α expression

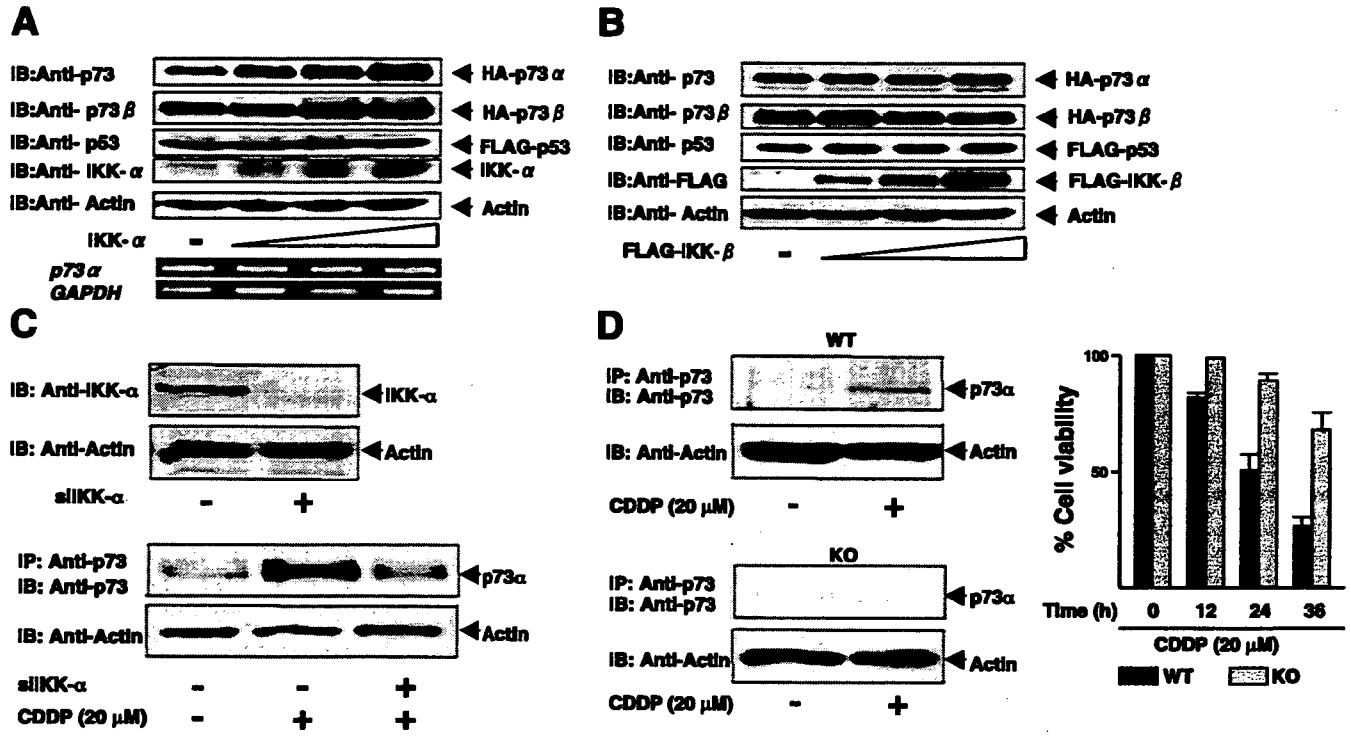

FIGURE 6. **IKK-α increases p73α stability.** *A*, the ectopic expression of IKK-α increases the stability of p73, but not of p53. COS-7 cells were transiently cotransfected with the indicated combinations of expression plasmids. Whole cell lysates and total RNA were prepared and subjected to immunoblotting (*IB*) (*upper panels*) or RT-PCR (*lower panels*), respectively. *GAPDH*, glyceraldehyde-3-phosphate dehydrogenase. *B*, IKK-β does not affect the stability of p73. COS-7 cells were transiently cotransfected with the indicated combinations of expression plasmids. Whole cell lysates were subjected to immunoblotting with the indicated antibodies. *C*, the reduction of endogenous IKK-α results in the attenuation of the CDDP-mediated accumulation of p73α. U2OS cells were transiently transfected with the expression plasmid for siRNA against IKK-α (*siIKK-α*) or with the scrambled control. Forty-eight hours after transfection, whole cell lysates were analyzed by immunoblotting with anti-IKK-α antibody. *Upper panels*, actin levels were used to monitor loading. *Lower panels*, U2OS cells were transiently transfected with the expression plasmid as in the *upper panels*. Twenty-four hours after transfection, cells were exposed to CDDP (at a final concentration of 20 μM) for 36 h or left untreated. Equal amounts of whole cell lysates were subjected to immunoprecipitation with anti-p73 antibody, followed by immunoblotting with anti-p73 antibody. Actin was included as a loading control. *D*, the CDDP-mediated accumulation of p73α is not detectable in IKK-$\alpha^{-/-}$ MEFs. Wild-type (*WT*) and IKK-$\alpha^{-/-}$ MEFs were treated with or without CDDP (at a final concentration of 20 μM) for 24 h. Equal amounts of whole cell lysates were subjected to immunoprecipitation (*IP*) with anti-p73 antibody, followed by immunoblotting with anti-p73 antibody. *Left panels*, actin was included as a loading control. *Right panel*, shown are the results of MTT assay. Wild-type and IKK-$\alpha^{-/-}$ MEFs were treated with CDDP (at a final concentration of 20 μM). At the indicated time periods after CDDP treatment, their viability was examined by MTT assay. *KO*, knock-out.

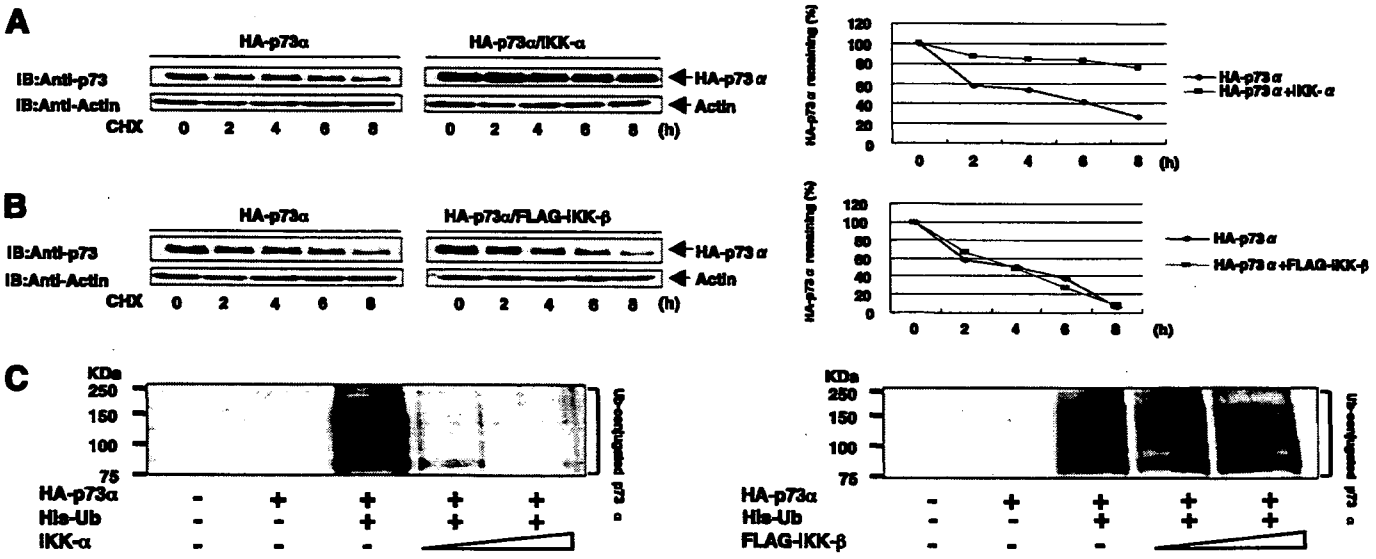

FIGURE 7. **IKK-α increases the half-life of p73α.** *A* and *B*, IKK-α or the FLAG-IKK-β expression plasmid, respectively, was transiently transfected into COS-7 cells with the expression plasmid for HA-p73α for 24 h. Cells were treated with cycloheximide (*CHX*) and harvested at the indicated time periods, followed by immunoblotting (*IB*) with anti-p73 antibody. The intensity of the bands was quantified by densitometry, and the HA-p73α remaining is indicated graphically. *C*, IKK-α inhibits the ubiquitination of p73. COS-7 cells were transiently cotransfected with the indicated combinations of expression plasmids and treated with MG132. Ubiquitinated products were recovered on nickel-agarose beads and separated by SDS-PAGE, followed by immunoblotting with anti-HA antibody. The *brackets* indicate slowly migrating ubiquitinated (*Ub*) forms of HA-p73α.

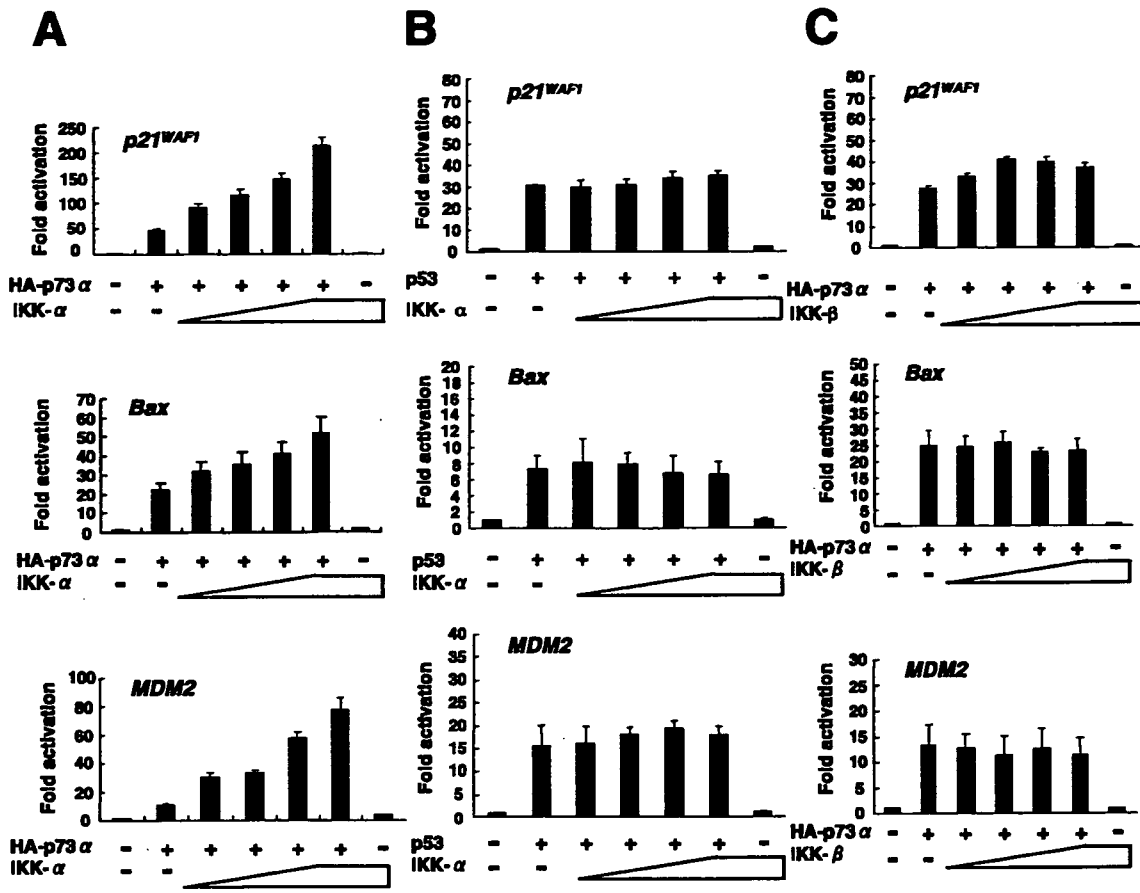

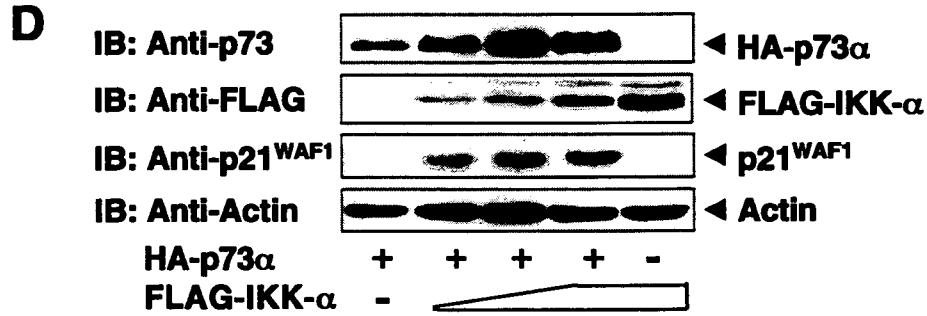

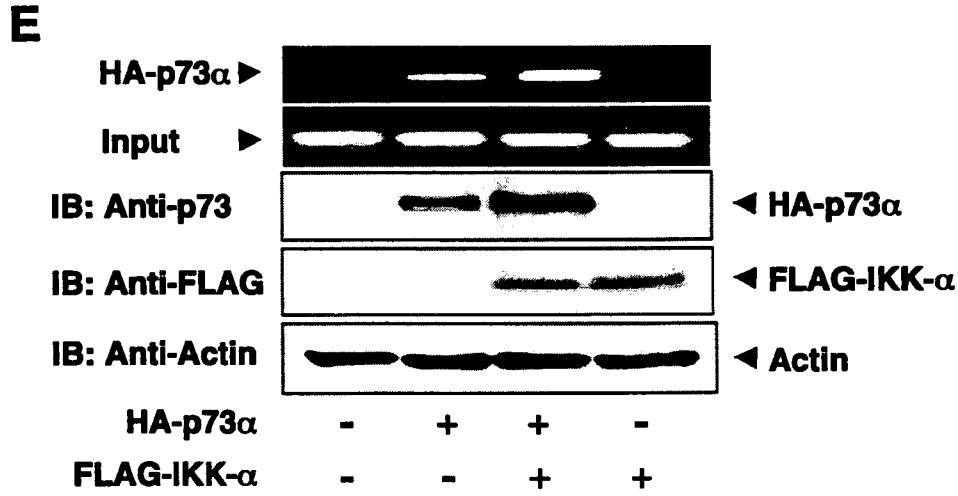

markedly inhibited the CDDP-mediated accumulation of p73α. To further confirm the effects of endogenous IKK-α, wild-type and IKK-$\alpha^{-/-}$ MEFs were treated with or without CDDP for 24 h, and whole cell lysates were immunoprecipitated with anti-p73 antibody. As expected, CDDP-mediated accumulation of endogenous p73α was detected in wild-type, but not IKK-$\alpha^{-/-}$, MEFs, and CDDP sensitivity was decreased in IKK-$\alpha^{-/-}$ MEFs compared with wild-type MEFs (Fig. 6*D*).

To explore whether IKK-α can modulate p73 turnover, we examined the decay rate of p73α in COS-7 cells. Twenty-four hours after transfection, cells were treated with cycloheximide. At the indicated time points, whole cell lysates were prepared and subjected to immunoblotting with anti-p73 antibody. As shown in Fig. 7*A*, the degradation rate of HA-p73α was slower in cells expressing both HA-p73α and IKK-α than that in cells expressing HA-p73α alone. In contrast, the half-life of HA-p73α was not prolonged in the presence of FLAG-IKK-β (Fig. 7*B*). An IKK-α-mediated increase in the half-life of endogenous p73α was also observed. Thus, IKK-α-mediated p73α stabilization resulted from the increase in the half-life of p73α. As described previously (43), the steady-state level of p73 is regulated at least in part by the protein degradation process through the ubiquitin/proteasome pathway. We then determined whether IKK-α can inhibit the ubiquitination of p73. To this end, COS-7 cells were transiently cotransfected with the expression plasmids for HA-p73α and His-ubiquitin with or without increasing amounts of the expression plasmid for IKK-α or FLAG-IKK-β. Forty-eight hours after transfection, whole cell lysates were prepared and analyzed by immunoblotting for the presence of His-ubiquitin-containing p73α. As shown in Fig. 7*C*, the amounts of the ubiquitinated forms of p73α were decreased in the presence of IKK-α, whereas FLAG-IKK-β inhibited the ubiquitination of p73α to a lesser degree. Taken together, these results strongly suggest that IKK-α inhibits the ubiquitination of p73α, thereby increasing the stability of p73α.

IKK-α Enhances p73-mediated Transactivation and Pro-apoptotic Functions in p53-deficient H1299 Cells—To address the functional implications of the interaction between IKK-α and p73, we first examined the effects of IKK-α on p73-mediated transcriptional activation. To this end, we cotransfected p53-deficient H1299 cells with the HA-p73α expression plasmid and the luciferase reporter construct under the control of the p21^{WAF1}, *bax*, or *MDM2* promoter with or without increasing amounts of the expression plasmid encoding IKK-α. As shown in Fig. 8*A*, ectopically expressed p73α successfully activated the transcription of each of these p53/p73-responsive reporters compared with the empty control plasmids, and IKK-α alone had little effect on luciferase activity. When HA-p73α was coexpressed with IKK-α, a marked increase in p73α-dependent transcriptional activation was observed in a dose-dependent manner. IKK-α also enhanced p73β-mediated transcriptional activation (data not shown). In contrast, there was no detectable IKK-α-induced increase in p53-dependent reporter gene activity (Fig. 8*B*). To examine the specificity of the IKK-α-mediated activation of p73-dependent transcription, we investigated whether IKK-β can enhance p73 transcriptional activity for the p53/p73-responsive promoters. As shown in Fig. 8*C*, no significant changes in p73α-dependent transcriptional activation were found with FLAG-IKK-β. In addition, the ectopic expression of IKK-α had no detectable effects on luciferase activity in p73-deficient neuroblastoma SK-N-AS cells bearing a mutant form of p53 (15, 44). Furthermore, the exogenous expression of IKK-α in H1299 cells resulted in a significant up-regulation of the p73α-mediated induction of endogenous p21^{WAF1} (Fig. 8*D*). To address whether the amounts of p73α associated with the p53/p73-responsive promoter can be increased in the presence of exogenous IKK-α, H1299 cells were transiently cotransfected with the expression plasmid for HA-p73α with or without the FLAG-IKK-α expression plasmid and subjected to chromatin immunoprecipitation analysis. As shown in Fig. 8*E*, the IKK-α-inducible association of p73α with the *bax* promoter was detected. Taken together, these results strongly suggest that IKK-α specifically enhances the transcriptional activity of p73.

We next investigated the potential impact of IKK-α on p73-dependent biological functions such as the regulation of apoptosis. H1299 cells were transiently cotransfected with a constant amount of HA-p73α and β-galactosidase expression plasmids with or without increasing amounts of the expression plasmid for IKK-α or FLAG-IKK-β. The β-galactosidase expression plasmid was used to identify the transfected cells. Forty-eight hours after transfection, cells were subjected to double staining with trypan blue (nonviable cells) and Red-Gal (transfected cells), and the number of cells with purple coloration was scored as described previously (11). As shown in Fig. 9 (*A* and *B*), the coexpression of IKK-α with HA-p73α resulted in an increase in the number of apoptotic cells compared with the expression of HA-p73α alone. In contrast, the coexpression of FLAG-IKK-β had no significant effect on p73α-dependent apoptosis (Fig. 9*C*). These data are consistent with the positive effect of IKK-α on p73-dependent transcriptional activation.

Kinase-deficient Mutant IKK-α Fails to Stabilize p73—To examine whether the intrinsic kinase activity of IKK-α is required for the stabilization of p73, we generated a mutant form of IKK-α (IKK-α(K44A)) in which Lys^{44} within the ATP-binding motif was replaced with Ala. As described previously (45), mutation of this site impairs the kinase activity of IKK-α.

FIGURE 8. **IKK-α enhances the transcriptional activity of p73α.** *A* and *B*, p53-deficient H1299 cells were transiently cotransfected with the expression plasmid for HA-p73α or p53, respectively, with the indicated p53/p73 luciferase reporter construct in the presence or absence of the IKK-α expression plasmid, followed by reporter assay. *C*, IKK-β does not affect p73-mediated transcriptional activation. H1299 cells were transiently cotransfected with the expression plasmid encoding HA-p73α and the indicated reporter constructs with or without the IKK-β expression plasmid, followed by reporter assay. *D*, shown are the results from analysis of endogenous p21^{WAF1}. H1299 cells were transiently cotransfected with the indicated expression plasmids. Whole cell lysates were subjected to immunoblotting (*IB*) with the indicated antibodies. *E*, IKK-α increases the amount of p73α associated with the human *bax* promoter. H1299 cells were transiently cotransfected with the indicated combinations of expression plasmids. Forty-eight hours after transfection, cells were cross-linked with 1% formaldehyde and subjected to chromatin immunoprecipitation assays, followed by PCR analysis as described under "Experimental Procedures" (*upper panels*). Immunoblotting of the indicated proteins is also shown (*lower panels*).

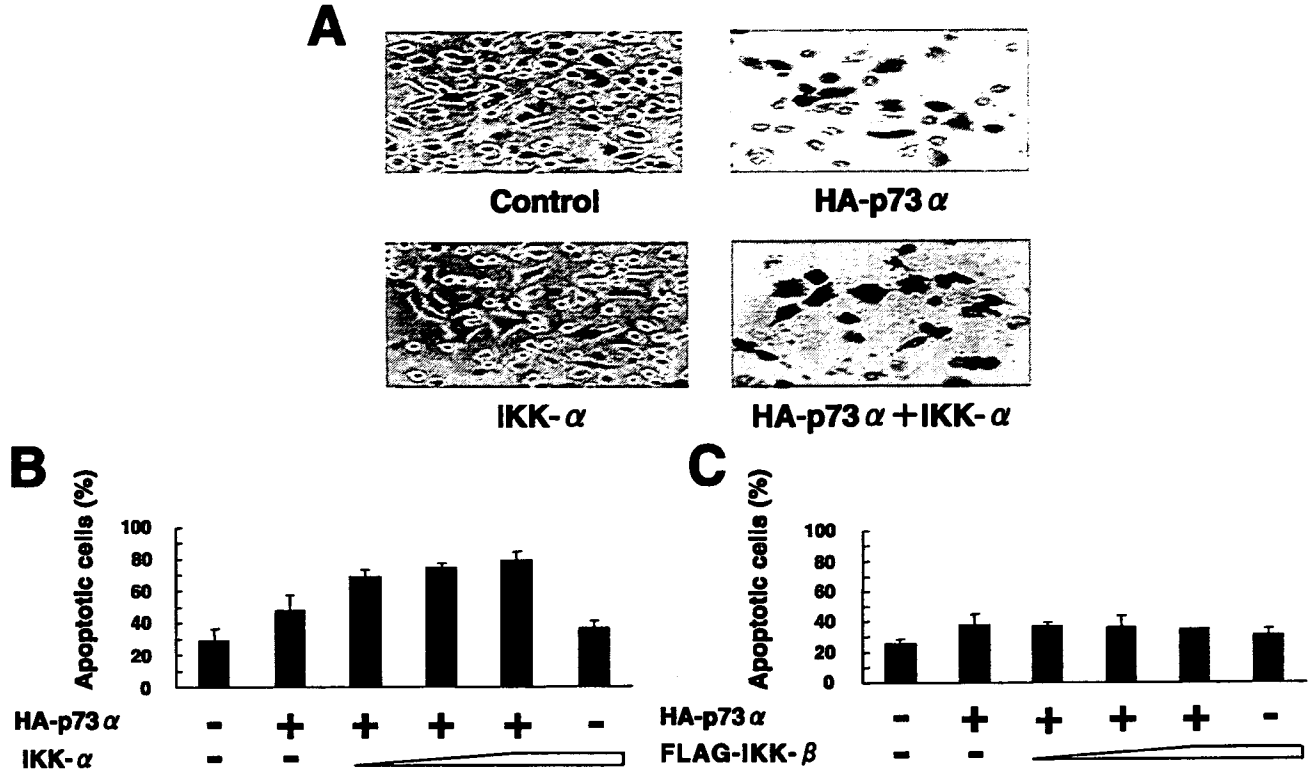

FIGURE 9. **IKK-α enhances the pro-apoptotic function of p73α.** *A* and *B*, H1299 cells were transiently cotransfected with the expression plasmids for HA-p73α and β-galactosidase with or without IKK-α. Control transfection was performed with the empty plasmid plus the β-galactosidase expression plasmid. Forty-eight hours after transfection, cells were double-stained with trypan blue (*blue*) and Red-Gal (*red*) (*A*), and the number of transfected cells (positive for β-galactosidase) and transfected apoptotic cells (*dark pink-purple*) in at least three different fields (>300 transfected cells) was measured. The percentage of transfected apoptotic cells is indicated (*B*). *C*, H1299 cells were transiently cotransfected with the indicated combinations of expression plasmids plus the β-galactosidase expression plasmid and processed for double staining as described above. The percentage of transfected apoptotic cells is indicated.

Immunoprecipitation analysis indicated that IKK-α(K44A) retained the ability to form a complex with p73α in cells (Fig. 10*A*). In sharp contrast to wild-type IKK-α, the coexpression of FLAG-IKK-α(K44A) had little or no effect on the intracellular level of exogenously expressed HA-p73α (Fig. 10*B*). To examine the effect of kinase-deficient IKK-α on endogenous p73, U2OS cells were transiently transfected with the empty plasmid or the FLAG-IKK-α(K44A) expression plasmid and then exposed to CDDP for 24 h or left untreated. Whole cell lysates and total RNA were prepared and subjected to immunoblotting and RT-PCR, respectively. As shown in Fig. 10*C*, the CDDP-mediated stabilization of endogenous p73α was markedly inhibited in U2OS cells transfected with the FLAG-IKK-α(K44A) expression plasmid, whereas FLAG-IKK-α(K44A) had no significant effect on the amount of endogenous p53. In good agreement with the observations above, CDDP-induced apoptosis was significantly inhibited in the presence of FLAG-IKK-α(K44A) (Fig. 10*D*). Similar results were also obtained in H1299 cells (Fig. 10, *E* and *F*). Thus, the kinase activity of IKK-α appears to be required for the stabilization of p73 in response to CDDP-induced DNA damage.

IKK-α Has the Ability to Phosphorylate p73—To address whether IKK-α can phosphorylate p73, we performed an *in vitro* kinase assay. GST alone or the indicated GST-p73 deletion mutants (Fig. 11) were incubated with the active form of IKK-α in the presence of [γ-^{32}P]ATP. After incubation, the reaction mixture was separated by SDS-PAGE, followed by autoradiography. As shown in Fig. 11, GST-p73-(1–62) was phosphorylated by IKK-α, suggesting that the N-terminal region of p73 is phosphorylated by the active form of IKK-α.

DISCUSSION

Until recently, the IKK complex has been thought to participate in the cytoplasmic signaling pathway that activates NF-κB. However, this viewpoint has been challenged with the findings of the nuclear accumulation and function of IKK-α in response to cytokine exposure (33, 34). According to the previous results, nuclear IKK-α contributes to the induction of NF-κB-dependent gene expression through histone H3 phosphorylation. In this study, we found that CDDP treatment (DNA cross-linking) leads to a remarkable accumulation of IKK-α in the cell nucleus. We also demonstrated that IKK-α directly binds to the sequence-specific DNA-binding domain of p73α and has positive effects on its stability as well as pro-apoptotic function. The CDDP-induced stabilization of p73α was dependent on IKK-α as examined by siRNA-mediated knockdown and using IKK-α$^{-/-}$ MEFs. In addition, chromatin immunoprecipitation assays showed that the IKK-α-dependent stabilization of p73α correlates with an increase in the amounts of p73α recruited onto the human *bax* promoter. Our present findings therefore imply not only a novel nuclear role of IKK-α in regulating the DNA damage response, which is distinct from NF-κB activation, but also a new regulatory pathway of pro-apoptotic p73α.

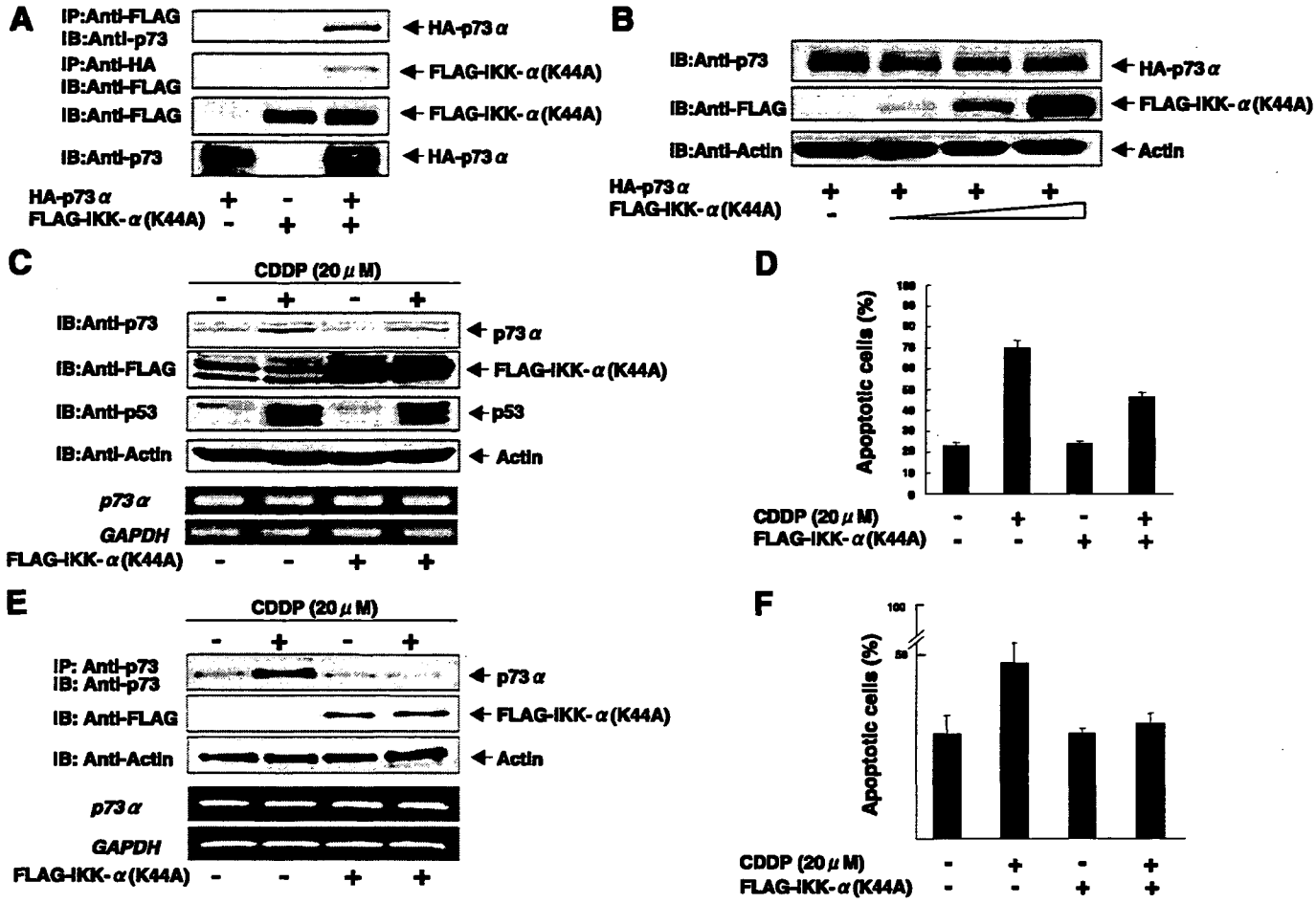

FIGURE 10. **Kinase-deficient IKK-α fails to stabilize p73α.** *A*, shown is the physical interaction between IKK-α(K44A) and p73α. COS-7 cells were transiently cotransfected with the indicated expression plasmids. Whole cell lysates were subjected to immunoprecipitation (*IP*) with anti-FLAG or anti-HA antibody, followed by immunoblotting (*IB*) with anti-p73 or anti-FLAG antibody, respectively. *B*, IKK-α(K44A) has no detectable effect on the amount of p73α. COS-7 cells were transiently cotransfected with the indicated combinations of expression plasmids. Equal amounts of the lysates were subjected to immunoblotting with anti-p73 or anti-FLAG antibody. *C*, IKK-α(K44A) suppresses endogenous p73 in response to CDDP. U2OS cells transiently transfected with or without FLAG-IKK-α(K44A) were left untreated or treated with CDDP for 24 h. Whole cell lysates and total RNA were prepared and subjected to immunoblotting (*upper panels*) or RT-PCR analysis (*lower panels*). *GAPDH*, glyceraldehyde-3-phosphate dehydrogenase. *D*, IKK-α(K44A) inhibits CDDP-induced apoptosis. U2OS cells transiently cotransfected with the β-galactosidase expression plasmid with or without the FLAG-IKK-α(K44A) expression plasmid were treated with CDDP for 24 h or left untreated. Cells were then subjected to double staining as described in the legend to Fig. 9. The percentage of transfected apoptotic cells is indicated. *E* and *F*, transfected H1299 cells were exposed to CDDP or left untreated and subjected to immunoprecipitation, followed by immunoblotting (*E*, *upper panels*), RT-PCR (*E*, *lower panels*), and apoptosis assays (*F*).

Previous studies have suggested that endogenous p73 is both stabilized and activated for apoptosis in response to CDDP and γ-ionizing irradiation through a pathway that depends on the nuclear non-receptor tyrosine kinase c-Abl (15–17). c-Abl binds to p73 via the P*XX*P motif of p73 and the c-Abl SH3 (Src homology 3) domain and phosphorylates p73 at Tyr^{99}. The phosphorylated form of p73 undergoes nuclear redistribution and becomes associated with the nuclear matrix in a c-Abl-dependent manner (36). In addition, HIPK2 (homeodomain-interacting protein kinase-2), which interacts with p73 and enhances its function, co-localizes with p73 in nuclear body-like structures (46). Mittnacht and Weinberg (47) reported that the retinoblastoma protein pRb differentially associates with the nuclear matrix, depending on its phosphorylation status or the integrity of the protein. The underphosphorylated form of pRb, which is active in growth control, remains tightly associated with the nuclear matrix, whereas the hyperphosphorylated form and a mutant form are detected largely in the nucleoplasm. In this study, we have demonstrated that IKK-α has the ability to stabilize and activate p73α and co-localizes with p73α in the nuclear lamina. Our findings, together with those previous observations, suggest that the nuclear structures including the nuclear matrix and/or nuclear body might provide an important subnuclear locale for p73 function.

As expected from their extensive amino acid sequence similarity, both IKK-α and IKK-β display IκB kinase activity *in vitro* (48), suggesting that their biochemical and biological functions seem to be redundant and overlapping with regard to NF-κB activation. On the other hand, genetic disruption studies in mice have demonstrated that IKK-α and IKK-β might have distinct regulatory functions. In IKK-α-deficient mice, inflammatory cytokine-induced activation of the NF-κB pathway is not severely impaired, although various developmental abnormalities, including defective epidermal differentiation, are detected (49–52). In contrast, mice lacking IKK-β die immedi-

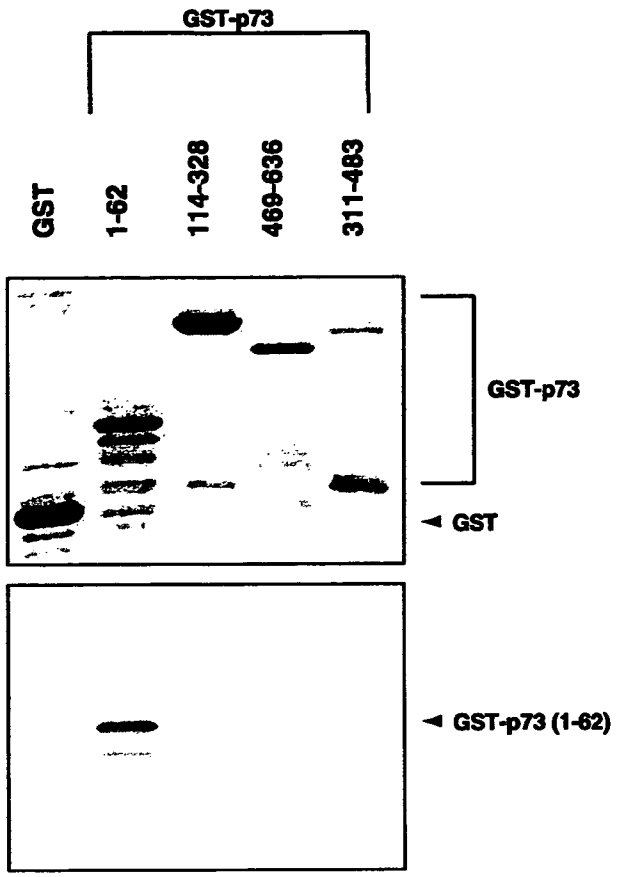

FIGURE 11. **Active form of IKK-α phosphorylates p73 *in vitro*.** Shown is the expression of GST-p73 deletion mutants. *Upper panel*, purified GST and the indicated GST-p73 deletion mutants were analyzed by SDS-PAGE, followed by Coomassie Brilliant Blue staining. *Lower panel*, shown are the results from the *in vitro* kinase reaction. Equal amounts of GST and the indicated GST-p73 deletion mutants were incubated with the active form of IKK-α in the presence of [γ-^{32}P]ATP. After incubation, the reaction mixtures were separated by SDS-PAGE and subjected to autoradiography.

ately after birth because of uncontrolled hepatic apoptosis and exhibit an extensive defect in the activation of the NF-κB pathway (49). Thus, it is likely that IKK-β is absolutely critical in the regulation of inducible IκB degradation and the subsequent activation of the NF-κB pathway in response to inflammatory stimuli, whereas IKK-α is not required for this process. Alternatively, other studies suggest that IKK-α is involved in NF-κB activation through a second pathway that leads to the processing of the NF-κB2 (p100) precursor (53, 54). Under our experimental conditions, IKK-β bound to p73α as determined by immunoprecipitation analysis (data not shown); however, it failed to stabilize p73α and to enhance its transactivation as well as pro-apoptotic activity. Unlike IKK-α, the amounts of endogenous nuclear IKK-β remained almost unchanged in response to CDDP. This is in good agreement with recent observations showing that IKK-α, but not IKK-β, has the ability to shuttle between the nucleus and cytoplasm (32). Taken together, our findings suggest that their functional divergence might be attributed at least in part to their differential interaction with p73.

Another finding of this study is that CDDP treatment results in a marked phosphorylation of IκB-α in association with a significant down-regulation of cytoplasmic IκB-α; however, the amounts of nuclear p65 remains unchanged. Consistent with these results, CDDP treatment did not enhance NF-κB transcriptional activity in U2OS cells; however, p65 was induced to accumulate in the nucleus of L929 cells in response to TNF-α. Bian *et al.* (13) also reported that no change in NF-κB-dependent transcriptional activation is observed in certain neuroblastoma cells in response to CDDP. It is therefore likely that, during the CDDP-dependent apoptotic process, the survival pathway mediated by NF-κB might be impaired. As described previously (55), nuclear c-Abl is activated by DNA-damaging agents, including CDDP, but not by TNF-α, indicating that the differential behavior of p65 in response to CDDP or TNF-α might be due to the presence or absence of the activated form of c-Abl, respectively. In sharp contrast to CDDP, various anticancer agents, including camptothecin (topoisomerase I inhibition), paclitaxel (microtubule depolymerization inhibition), and doxorubicin (topoisomerase II inhibition), significantly induce the down-regulation of IκB-α and promote the nuclear translocation of NF-κB, followed by subsequent NF-κB-dependent transcriptional activation (13, 56, 57). Considering that the cytoplasmic retention of NF-κB by IκB is the major molecular mechanism that controls its activity as well as cell fate determination (reviewed in Ref. 3), the CDDP-mediated attenuation of the nuclear accumulation of p65 might be required at least in part for apoptotic cell death in response to CDDP. In this connection, it is worth noting that NF-κB promotes T cell survival by reducing the transcription of *p73* following antigenic stimulation (27). Currently, it is not clear how the nuclear accumulation of p65 is blocked in cells exposed to CDDP, even though cytoplasmic IκB-α is significantly decreased in our system. Future experiments will be necessary to clarify the underlying mechanistic details of this phenomenon.

It has been shown that p73 stability is regulated in a ubiquitination-dependent and -independent manner (43, 58). p73 is stabilized by coexpression with c-Abl or protein kinase Cδ, which phosphorylates p73 at Tyr^{99} or Ser^{289}, respectively (16, 42). According to our results, IKK-α had the ability to stabilize p73, whereas the kinase-deficient mutant form of IKK-α does not, suggesting that the kinase activity of IKK-α is required for the stabilization of p73. As described previously (reviewed in Ref. 59), the amino acid sequence DSGΨ*X*S (where Ψ is a hydrophobic amino acid and *X* is any amino acid) has been identified as a consensus motif for the IKK-dependent phosphorylation of IκB proteins. During the search for a putative phosphorylation site(s) targeted by IKK within the amino acid sequence of p73α, we failed to find a related motif. Of note, it has been shown that IKK-α, but not IKK-β and the kinase-deficient IKK-α mutant, phosphorylates histone H3 at Ser^{10}, which has no IKK phosphorylation consensus sequence (33, 34). According to our *in vitro* kinase reaction, the active form of IKK-α has the ability to phosphorylate the N-terminal region of p73α. Because IKK-α, but not the kinase-deficient IKK-α mutant, has the ability to stabilize p73α, it is important to determine whether IKK-α can phosphorylate p73 in cells exposed to CDDP. In addition, it will be interesting to identify the signaling component(s) upstream of IKK-α that could receive the nuclear signal in response to CDDP-mediated DNA damage.

As described previously (60), the transcriptional coactivator p300 and CBP interact with p73 and enhance its function. Costanzo *et al.* (61) reported that DNA damage induces the acetylation of p73 by p300 in a c-Abl-dependent manner. In addition, Haupt *et al.* (62) found that p300-mediated acetylation results in p73 stabilization. It is worth noting that IKK-α, but not IKK-β, has the ability to interact with CBP (33). According to the previous results, IKK-α is required for the cytokine-induced phosphorylation and subsequent acetylation of histone H3. Although the precise molecular mechanism behind the IKK-α-dependent stabilization of p73 remains unknown, it is likely that a functional interaction might exist among c-Abl, p300/CBP, IKK-α, and p73. Our preliminary results suggest that the kinase-deficient form of c-Abl inhibits the IKK-α-dependent stabilization of p73α (data not shown). This issue is currently under investigation in our laboratory.

Upon CDDP treatment, endogenous p73α and p53 are significantly induced at the protein level in U2OS cells bearing wild-type *p53* (45). Unlike p73, p53 is targeted for degradation by MDM2 through the ubiquitination-dependent proteasome pathway (reviewed in Ref. 38). It is well known that, in response to DNA damage, p53 is phosphorylated at multiple sites, including Ser^{15} and Ser^{20}, and that these phosphorylation events stimulate p53 stabilization by preventing the interaction with MDM2. Alternatively, Li *et al.* (63) found that HAUSP (herpesvirus-associated ubiquitin-specific protease) participates in the deubiquitination and subsequent stabilization of p53. Because the kinase-deficient IKK-α mutant inhibited the CDDP-induced stabilization of endogenous p73, but not of p53, the IKK-α-dependent stabilization appears to be highly specific to p73. Recently, Rossi *et al.* (64) reported that the HECT-type ubiquitin-protein isopeptide ligase Itch binds to and ubiquitinates p73, but not p53. Their study demonstrated that CDDP treatment results in a rapid reduction of Itch protein levels, indicating that Itch could contribute to the IKK-α-mediated stabilization of p73α.

Furthermore, it has been shown that p53-dependent apoptosis requires the indirect contribution of at least one of the other p53 family members, p73 or p63, whereas p73 is sufficient in the absence of p53 to induce apoptosis (65). *p53* is the most frequent target for genetic alterations in human cancers, leading to loss of its pro-apoptotic function (66). In addition to mutation of *p53* itself, many cancers bearing wild-type *p53* may harbor the other defects in the p53 pathway (reviewed in Ref. 38). In contrast to *p53*, *p73* is infrequently mutated in many human cancers (67). Given the specific induction and activation of p73 by IKK-α, it is likely that the IKK-α-mediated induction of p73 substitutes for the downstream defects in the p53 pathway and/or enables p53 to cooperate with p73 to induce apoptosis.

Acknowledgments—We express our sincere appreciation to Drs. K. Takeshige and T. Muta for pELAM1-Luc. We give special thanks to Dr. Michael Karin for providing IKK-$\alpha^{-/-}$ MEFs. We thank S. Ono for excellent technical assistance.

REFERENCES

1. Li, Q., and Verma, I. M. (2002) *Nat. Rev. Immunol.* 2, 725–734
2. Karin, M. (2006) *Nature* **441**, 431–436
3. Karin, M., and Ben-Neriah, Y. (2000) *Annu. Rev. Immunol.* **18**, 621–663
4. Beg, A. A., and Baltimore, D. (1996) *Science* **274**, 782–784
5. Liu, Z., Hsu, G. H., Goeddel, D. V., and Karin, M. (1996) *Cell* **87**, 565–576
6. Wang, C.-Y., Mayo, M. W., and Baldwin, A. S., Jr. (1996) *Science* **274**, 784–787
7. Van Antwerp, D. J., Martin, S. J., Kafri, T., Green, D. R., and Verma, I. M. (1996) *Science* **274**, 787–789
8. Wang, C.-Y., Mayo, M. W., Korneluk, R. G., Goeddel, D. V., and Baldwin, A. S., Jr. (1998) *Science* **281**, 1680–1683
9. Wang, C.-Y., Cusack, J. C., Jr., Liu, R., and Baldwin, A. S., Jr. (1999) *Nat. Med.* **5**, 412–417
10. Cusack, J. C., Jr., Liu, R., Houston, M., Abendroth, K., Elliott, P. J., Adams, J., and Baldwin, A. S., Jr. (2001) *Cancer Res.* **61**, 3535–3540
11. Bayon, Y., Ortiz, M. A., Lopez-Hernandez, F. J., Gao, F., Karin, M., Pfahl, M., and Piedrafita, F. J. (2003) *Mol. Cell. Biol.* **23**, 1061–1074
12. Huang, Y., and Fan, W. (2002) *Mol. Pharmacol.* **61**, 105–113
13. Bian, X., McAllister-Lucas, I. M., Shao, F., Schumacher, K. R., Feng, Z., Porter, A. G., Castle, V. P., and Opipari, A. W. (2001) *J. Biol. Chem.* **276**, 48921–48929
14. Melino, G., De Laurenzi, V., and Vousden, K. H. (2002) *Nat. Rev. Cancer* **2**, 605–615
15. Gong, J., Costanzo, A., Yang, H.-Q., Melino, G., Kaelin, W. G., Jr., Levreno, M., and Wang, J. Y. (1999) *Nature* **399**, 806–809
16. Agami, R., Blandino, G., Oren, M., and Shaul, Y. (1999) *Nature* **399**, 809–813
17. Yuan, Z.-M., Shioya, H., Ishiko, T., Sun, X., Gu, J., Huang, Y. Y., Lu, H., Kharbanda, S., Weichselbaum, R., and Kufe, D. (1999) *Nature* **399**, 814–817
18. Yang, A., Walker, N., Bronson, R., Kaghad, M., Oosterwegel, M., Bonnin, J., Vagner, C., Bonnet, H., Dikkens, P., Sharpe, A., McKeon, F., and Caput, D. (2000) *Nature* **404**, 99–103
19. Pozniak, C. D., Radinovic, S., Yang, A., McKeon, F., Kaplan, D. R., and Miller, F. D. (2000) *Science* **289**, 304–306
20. Stiewe, T., Zimmermann, S., Frilling, A., Esche, H., and Putzer, B. M. (2002) *Cancer Res.* **62**, 3598–3602
21. Grob, T. J., Novak, U., Maisse, C., Barcaroli, D., Luthi, A. U., Pirnia, F., Hugli, B., Graber, H. U., De Laurenzi, V., Fey, M. F., Melino, G., and Tobler, A. (2001) *Cell Death Differ.* **8**, 1213–1223
22. Nakagawa, T., Takahashi, M., Ozaki, T., Watanabe, K., Todo, S., Mizuguchi, H., Hayakawa, T., and Nakagawara, A. (2002) *Mol. Cell. Biol.* **22**, 2575–2585
23. Zaika, A. I., Slade, N., Erster, S. H., Sansome, C., Joseph, T. W., Pearl, M., Chalas, E., and Moll, U. M. (2002) *J. Exp. Med.* **196**, 765–780
24. Wan, Y. Y., and DeGregori, J. (2003) *Immunity* **18**, 331–342
25. Tergaonkar, V., Pando, M., Vafa, O., Wahl, G., and Verma, I. M. (2002) *Cancer Cell* **1**, 493–503
26. Chang, N.-S. (2002) *J. Biol. Chem.* **277**, 10323–10331
27. Ryan, K. M., Ernst, M. K., Rice, N. R., and Vousden, K. H. (2000) *Nature* **404**, 892–897
28. Wu, H., and Lozano, G. (1994) *J. Biol. Chem.* **269**, 20067–20074
29. Sun, X., Shimizu, H., and Yamamoto, K. (1995) *Mol. Cell. Biol.* **15**, 4489–4496
30. Hellin, A. C., Calmant, P., Gielen, J., Bours, V., and Mervillie, M. P. (1998) *Oncogene* **16**, 1187–1195
31. Fujioka, S., Schmidt, C., Sclabas, G. M., Li, Z., Pelicano, H., Peng, B., Yao, A., Niu, J., Zhang, W., Evans, D. B., Abbruzzese, J. L., Huang, P., and Chiao, P. J. (2004) *J. Biol. Chem.* **279**, 27549–27559
32. Birbach, A., Gold, P., Binder, B. R., Hofer, E., de Martin, R., and Schmid, J. (2002) *J. Biol. Chem.* **277**, 10842–10851
33. Yamamoto, Y., Verma, U. N., Prajapati, S., Kwak, Y.-T., and Gaynor, R. B. (2003) *Nature* **423**, 655–659
34. Anest, V., Hanson, J. L., Cogswell, P. C., Steinbrecher, K. A., Strahl, B. D., and Baldwin, A. S., Jr. (2003) *Nature* **423**, 659–663
35. Nickerson, J. A., Krockmalnic, G., Wan, K. M., Turner, C. D., and Penman, S. (1992) *J. Cell Biol.* **116**, 977–987
36. Ben-Yehoyada, M., Ben-Dor, I., and Shaul, Y. (2003) *J. Biol. Chem.* **278**, 34475–34482
37. Xirodimas, D., Staville, M. K., Edling, C., Lane, D. P., and Lain, S. (2001)

Oncogene **20,** 4972–4983
38. Vousden, K. H., and Lu, X. (2002) *Nat. Rev. Cancer* **2,** 594–604
39. Verma, U. N., Yamamoto, Y., Prajapati, S., and Gaynor, R. B. (2004) *J. Biol. Chem.* **279,** 3509–3515
40. Muta, T., and Takeshige, K. (2001) *Eur. J. Biochem.* **268,** 4580–4589
41. Hehner, S. P., Hofmann, T. G., Ratter, F., Dumont, A., Droge, W., and Schmitz, M. L. (1998) *J. Biol. Chem.* **273,** 18117–18121
42. Ren, J., Datta, R., Shioya, H., Li, Y., Oki, E., Biedermann, V., Bharti, A., and Kufe, D. (2002) *J. Biol. Chem.* **277,** 33758–33765
43. Lee, C.-W., and La Thangue, N. B. (1999) *Oncogene* **18,** 4171–4181
44. Nakamura, Y., Ozaki, T., Niizuma, H., Ohira, M., Kamijo, T., and Nakagawara, A. (2007) *Biochem. Biophys. Res. Commun.* **354,** 892–898
45. Ling, L., Cao, Z., and Goeddel, D. V. (1998) *Proc. Natl. Acad. Sci. U. S. A.* **95,** 3792–3797
46. Kim, E.-J., Park, J.-S., and Um, S.-J. (2002) *J. Biol. Chem.* **277,** 32020–32028
47. Mittnacht, S., and Weinberg, R. A. (1991) *Cell* **65,** 381–393
48. Zandi, E., Chen, Y., and Karin, M. (1998) *Science* **281,** 1360–1363
49. Li, Q., Van Antwerp, D., Mercurio, F., Lee, K. F., and Verma, I. M. (1999) *Science* **284,** 321–325
50. Takeda, K., Takeuchi, O., Tsujimura, T., Itami, S., Adachi, O., Kawai, T., Sanjo, H., Yoshikawa, K., Terada, N., and Akira, S. (1999) *Science* **284,** 313–316
51. Hu, Y., Baud, V., Delhase, M., Zhang, P., Deerinck, T., Ellisman, M., Johnson, R., and Karin, M. (1999) *Science* **284,** 316–320
52. Li, Q., Lu, Q., Hwang, J. Y., Buscher, D., Lee, K. F., Izpisua-Belmonte, J. C., and Verma, I. M. (1999) *Genes Dev.* **13,** 1322–1328
53. Senftleben, U., Cao, Y., Xiao, G., Greten, F. R., Krahn, G., Bonizzi, G., Chen, Y., Hu, Y., Fong, A., Sun, S. C., and Karin, M. (2001) *Science* **293,** 1495–1499
54. Pomerantz, J. L., and Baltimore, D. (2002) *Mol. Cell* **10,** 693–695
55. Kharbanda, S., Ren, R., Pandey, P., Shafman, T. D., Feller, S. M., Weichselbaum, R. R., and Kufe, D. W. (1995) *Nature* **376,** 785–788
56. Huang, Y., Johnson, K. R., Norris, J. S., and Fan, W. (2000) *Cancer Res.* **60,** 4426–4432
57. Huang, T. T., Wuerzberger-Davis, S. M., Seufzer, B. J., Shumway, S. D., Kurama, T., Boothman, D. A., and Miyamoto, S. (2000) *J. Biol. Chem.* **275,** 9501–9509
58. Ohtsuka, T., Ryu, Y. H., Minamishima, Y. A., Ryo, A., and Lee, S. W. (2003) *Oncogene* **22,** 1678–1687
59. Karin, M. (1999) *Oncogene* **18,** 6867–6874
60. Zeng, X., Li, X., Miller, A., Yuan, Z., Yuan, W., Kwok, R. P. S., Goodman, R., and Lu, H. (2000) *Mol. Cell. Biol.* **20,** 1299–1310
61. Costanzo, A., Merlo, P., Pediconi, N., Fulco, M., Sartorelli, V., Cole, P. A., Fontemaggi, G., Fanciulli, M., Schiltz, L., Blandino, G., Balsano, C., and Levrero, M. (2002) *Mol. Cell* **9,** 175–186
62. Haupt, Y., Maya, R., Kazaz, A., and Oren, M. (1997) *Nature* **387,** 296–299
63. Li, M., Chen, D., Shiloh, A., Luo, J., Nikolaev, A. Y., Qin, J., and Gu, W. (2002) *Nature* **416,** 643–653
64. Rossi, M., De Laurenzi, V., Munarriz, E., Green, D. R., Liu, Y. C., Vousden, K. H., Cesareni, G., and Melino, G. (2005) *EMBO J.* **24,** 836–848
65. Flores, E. R., Tsai, K. Y., Crowley, D., Senqupta, S., Yang, A., McKeon, F., and Jacks, T. (2002) *Nature* **416,** 560–564
66. Hollstein, M., Soussi, T., Thomas, G., von Breven, M., and Bartsch, H. (1997) *Recent Results Cancer Res.* **143,** 369–389
67. Ikawa, S., Nakagawara, A., and Ikawa, Y. (1999) *Cell Death Differ.* **6,** 1154–1161

THE JOURNAL OF BIOLOGICAL CHEMISTRY VOL. 282, NO. 31, pp. 22993–23004, August 3, 2007

NFBD1/MDC1 Associates with p53 and Regulates Its Function at the Crossroad between Cell Survival and Death in Response to DNA Damage*[S]

Received for publication, December 13, 2006, and in revised form, May 2, 2007 Published, JBC Papers in Press, May 29, 2007, DOI 10.1074/jbc.M611412200

Mitsuru Nakanishi[‡§1], Toshinori Ozaki[‡1], Hideki Yamamoto[‡], Takayuki Hanamoto[‡], Hironobu Kikuchi[‡], Kazushige Furuya[‡], Masahiro Asaka[§], Domenico Delia[¶], and Akira Nakagawara[‡2]

From the [‡]Division of Biochemistry, Chiba Cancer Center Research Institute, Chiba 260-8717, Japan, the [§]Department of Gastroenterology, Hokkaido University School of Medicine, Sapporo 060-8638, Japan, and the [¶]Department of Experimental Oncology, Istituto Nazionale Tumori, 20133 Milan, Italy

NFBD1/MDC1, which belongs to the BRCT superfamily, has an anti-apoptotic activity and contributes to the early cellular responses to DNA damage. Here we found that NFBD1 protects cells from apoptotic cell death by inhibiting phosphorylation of p53 at Ser-15 under steady state as well as early phase of DNA damage, thereby blocking its transcriptional and pro-apoptotic activities. During late phase of DNA damage, a remarkable reduction of NFBD1 was observed in dying but not in surviving A549 cells bearing wild-type *p53*. Small interference RNA-mediated knockdown of the endogenous NFBD1 resulted in an increase in sensitivity to adriamycin in A549 cells but not in p53-deficient H1299 cells. Immunoprecipitation and luciferase reporter analyses demonstrated that NFBD1 binds to the NH_2-terminal region of p53 and strongly inhibits its transcriptional activity. Additionally, BRCT domains, which can interact with p53, reduced the adriamycin-induced phosphorylation levels of p53 at Ser-15 and also suppressed the transcriptional activity of p53. Thus, our present findings strongly suggest that NFBD1 plays an important role in the decision of cell survival and death after DNA damage through the regulation of p53.

The BRCA1 carboxyl terminus (BRCT)[3] domain is defined by distinct hydrophobic clusters of amino acids and is often found in a variety of cellular proteins such as BRCA1, 53BP1, and RAD9, which are involved in DNA repair and/or DNA damage signaling pathways (1–3). Although the functional role of the BRCT domain is currently unclear, the early works indicated that the BRCT domains of BRCA1 act as a transactivator (4, 5). Consistent with this notion, the point mutations detected within the BRCT domains of BRCA1 markedly inhibited its transcriptional activity (4, 5), and BRCA1 was a component of RNA polymerase II holoenzyme (6). Alternatively, the BRCT domains function as protein-protein interaction modules (7). For example, the BRCT domains of BRCA1 as well as 53BP1 were required for the interaction with p53 (8, 9).

NFBD1/MDC1 (nuclear factor with BRCT domain 1/mediator of DNA damage checkpoint protein 1) is a large nuclear protein bearing three characteristic structural domains, including an NH_2-terminal forkhead-associated (FHA) domain, an internal PST (proline/serine/threonine-rich) repeat domain, and tandem repeat of COOH-terminal BRCT domains (10–14). We have initially reported that NFBD1 acts as a nuclear transcriptional factor with an anti-apoptotic function (11). In accordance with our results, siRNA-mediated knockdown of NFBD1 led to a significant increase in the number of apoptotic cells (15). In addition, the elimination of NFBD1 expression increased the sensitivity to irradiation (16). These observations indicate that NFBD1 has an anti-apoptotic function; however, the precise molecular mechanisms behind the anti-apoptotic effect of NFBD1 remain to be explored.

Previous studies strongly suggest that NFBD1 is closely involved in early cellular responses to genotoxic stress. Upon DNA damage, NFBD1 was phosphorylated in an ATM/Chk2-dependent manner and cooperated with γH2AX to recruit DNA repair proteins to the sites of DNA damage (12–14). Consistent with this notion, NFBD1 was associated with the DNA double strand break repair MRN complex, including MRE11, RAD50, and NBS1, and also co-localized with the MRN complex as well as γH2AX at the nuclear foci in response to DNA damage (12, 14, 15, 17). Deletion analysis revealed that the FHA and BRCT domains of NFBD1 are required for the binding to the MRN complex and γH2AX, respectively (15). Furthermore, siRNA-mediated knockdown of NFBD1 led to a significant decrease in the number of irradiation-induced NBS1 foci (14), and the FHA and BRCT domains of NFBD1 were responsible for the formation of irradiation-induced nuclear foci contain-

* This work was supported in part by a grant-in-aid from the Ministry of Health, Labor, and Welfare for Third Term Comprehensive Control Research for Cancer, a grant-in-aid for Cancer Research from the Ministry of Health, Labor, and Welfare of Japan, a grant-in-aid from the Ministry of Education, Culture, Sports, Science and Technology, Japan, and a grant from Uehara Memorial Foundation. The costs of publication of this article were defrayed in part by the payment of page charges. This article must therefore be hereby marked "*advertisement*" in accordance with 18 U.S.C. Section 1734 solely to indicate this fact.

[S] The on-line version of this article (available at http://www.jbc.org) contains supplemental Fig. 1.

[1] Both authors contributed equally to this work.

[2] To whom correspondence should be addressed. Tel.: 81-43-264-5431; Fax: 81-43-265-4459; E-mail: akiranak@chiba-cc.jp.

[3] The abbreviations used are: BRCT, BRCA1 carboxyl terminus; ADR, adriamycin; ATM, ataxia-telangiectasia-mutated; CDDP, cisplatin; CPT-11, camptothecin; DAPI, 4,6-diamidino-2-phenylindole; FHA, forkhead-associated; GAPDH, glyceraldehyde-3-phosphate dehydrogenase; GFP, green fluorescent protein; HRP, horseradish peroxidase; MRN, MRE11-RAD50-NBS1; NFBD1, nuclear factor with BRCT domain 1; NF-κB, nuclear factor-κB; NRS, normal rabbit serum; NOX, nocodazole; PST, proline/serine/threonine-rich; PTX, paclitaxel; RT, reverse transcription; siRNA, small interference RNA; VP-16, etoposide; E3, ubiquitin-protein isopeptide ligase; MTT, 3-(4,5-dimethylthiazol-2-yl) 2,5-diphenyl-tetrazolium bromide.

ing NFBD1 (12–14). Lou *et al.* (18) described that the PST domain of NFBD1 binds to Ku/DNA-dependent protein kinase, and this interaction is critical for the efficient irradiation-induced autophosphorylation of DNA-dependent protein kinase.

p53 is a nuclear transcription factor with a pro-apoptotic function. In response to a wide variety of cellular stresses, including genotoxic stress, p53 is phosphorylated, and its half-life is dramatically prolonged. During the DNA damage-induced apoptosis, p53 is directly phosphorylated at Ser-15 and Ser-20 by ATM and Chk2, respectively (19–23). Such phosphorylation events contribute to the increased stability and activity of p53 by facilitating its dissociation from E3 ubiquitin protein ligase MDM2 (reviewed in Ref. 24).

In this study, we demonstrate that NFBD1 abrogates the adriamycin (ADR)-mediated apoptosis through the inhibition of the transcriptional as well as pro-apoptotic activity of p53. Our present findings strongly suggest that NFBD1 plays a pivotal role in the regulation of cell survival and death after DNA damage.

EXPERIMENTAL PROCEDURES

Cell Culture and Transfection—COS7 and HEK293T cells were maintained in Dulbecco's modified Eagle's medium containing 10% heat-inactivated fetal bovine serum (Invitrogen) and penicillin (100 IU/ml)/streptomycin (100 μg/ml). A549 and H1299 cells were grown in RPMI 1640 medium with the same supplements. Where indicated, cells were treated with ADR. For transfection, COS7 cells were transfected with the indicated expression plasmids using FuGENE 6 transfection reagent (Roche Applied Science), except for A549 and H1299 cells, for which Lipofectamine 2000 transfection reagent (Invitrogen) was used.

Cell Survival Assay—Cell viability was determined by a modified 3-(4,5-dimethylthiazol-2-yl) 2,5-diphenyl-tetrazolium bromide (MTT) assay. In brief, A549 cells were cultured overnight at 5×10^3 cells per well in a 96-well plate, and then exposed to ADR. At the indicated time periods after the treatment with ADR, 10 μl of MTT solution was added to each culture, and the mixture was maintained for another 3 h at 37 °C. The absorbance readings for each well were carried out at 570 nm using the microplate reader (model 450; Bio-Rad).

Isolation of RNA and RT-PCR—Total RNA was prepared from A549 cells using the RNeasy Mini kit (Qiagen, Valencia, CA) according to the manufacturer's protocol. A total of 1 μg of total RNA was used to generate cDNAs with random primers by SuperScript IIreverse transcriptase (Invitrogen). PCR amplification was carried out under standard conditions with rTaq DNA polymerase (Takara, Ohtsu, Japan). The primer sets used in this study were designed based on the cDNA sequences corresponding to each of the genes by using Primer3 software (Whitehead Institute). The primer sequences were as follows: $p21^{WAF1}$, 5′-ATGAAATTCACCCCCTTTCC-3′ (sense) and 5′-CCCTAGGCTGTGCTCACTTC-3′ (antisense); p53, 5′-GTCCAGATGAAGCTCCCAGA-3′ (sense) and 5′-CAAGGCCTCATTCAGCTCTC-3′ (antisense); NFBD1, 5′-AGCAACCCCAGTTGTCATTC-3′ (sense) and 5′-AGCGCTGCTGAGACTTCTTC-3′ (antisense); BAX, 5′-AGAGGATGATTGCCGCCGT-3′ (sense) and 5′-CAACCACCCTGGTCTTGGAT-3′ (antisense); PUMA, 5′-CTGTGAATCCTGTGCTCTGC-3′ (sense) and 5′-TCCTCCCTCTTCCGAGATTT-3′ (antisense); NOXA, 5′-CTGGAAGTCGAGTGTGCTACT-3′ (sense) and 5′-TCAGGTTCCTGAGCAGAAGAG-3′ (antisense); and GAPDH, 5′-ACCTGACCTGCCGTCTAGAA-3′ (sense) and 5′-TCCACCACCCTGTTGCTGTA-3′ (antisense). PCR products were separated by 1.5% agarose gel electrophoresis and stained with ethidium bromide.

Antibody Production—The cDNA sequence encoding the NH_2-terminal region of human NFBD1 (amino acid residues 1–150) was subcloned into the bacterial expression plasmid pGEX-4T-2 (Amersham Biosciences), expressed in *Escherichia coli* DH5α, and purified with a glutathione-Sepharose 4B column. The antiserum against NFBD1 was produced by immunizing rabbit with the above purified glutathione *S*-transferase fusion protein.

Construction of the Deletion Mutants of NFBD1—*NFBD1* cDNA fragment encoding NH_2-terminal FHA domain (amino acid residues 2–141), central PST domain (amino acid residues 788–1645), or COOH-terminal BRCT domains (amino acid residues 1858–2068) was amplified by PCR with the following primers: 5′-**GAATTC**GAGGACACCCAGGCTATT-3′ and 5′-**GAGCTC**AGTCCTCTGTTTCCCGTC-3′ or 5′-CCG**GAATTC**GACCAACATCCAGAGAGC-3′ and 5′-T**CGCCGG**CGAGTGAGTTCTAGTCTCCG-3′ or 5′-**GAATTC**AGCCTCCGACGCACCAAA-3′ or 5′-**GAGCTC**AGTACCTACTGTAGTGGT-3′, respectively. PCR primers also included 5′-EcoRI and 3′-XhoI or 5′-EcoRI and 3′-NotI restriction sites (boldface and underlined) to aid cloning. PCR products were then inserted in-frame into the appropriate restriction sites of the pcDNA3-FLAG to give pcDNA3-FLAG-FHA, pcDNA3-FLAG-PST, and pcDNA3-FLAG-BRCT.

RNA Interference—To construct an expression plasmid for siRNA against NFBD1, two DNA oligonucleotides were designed to produce 19-nucleotide siRNA. Oligonucleotides used are as follows: 5′-CCCCAGCTCGAGCCTTCCACTTCTTCAAGAGAGAAGTGGAAGGCTCGAGCTTTTTTGGAAAC-3′ and 5′-TCGAGTTTCCAAAAAAGCTCGAGCCTTCCACTTCTCTCTTGAAGAAGTGGAAGGCTCGAGCTGGGGAGCT-3′. These two oligonucleotides were mixed in equimolar amounts and annealed under the standard conditions. The annealed oligonucleotide was inserted into the SacI and XhoI restriction sites of pcDNA3 derivative in which the cytomegalovirus promoter was replaced with the *H1* promoter.

Generation of Stable A549 Cell Lines—To establish stable cell lines expressing siRNA against p53, A549 cells were stably transfected with pSUPER-p53 (OligoEngine, Seattle, WA) or with the backbone plasmid, and cultured in the presence of G418 (400 μg/ml). Two weeks after the selection in G418, drug-resistant clones were isolated and allowed to proliferate in medium containing G418.

Immunoblotting—Protein lysates (50 μg) were separated by 10% SDS-PAGE, electrotransferred onto Immobilon-P membranes (Millipore, Bedford, MA), and probed with anti-p53 (DO-1; Oncogene Research Products, Cambridge, MA), anti-FLAG (M2; Sigma), anti-BAX (6A7; eBioscience, San Diego), anti-GFP (1E4; MBL, Nagoya, Japan), anti-$p21^{WAF1}$ (H-164;

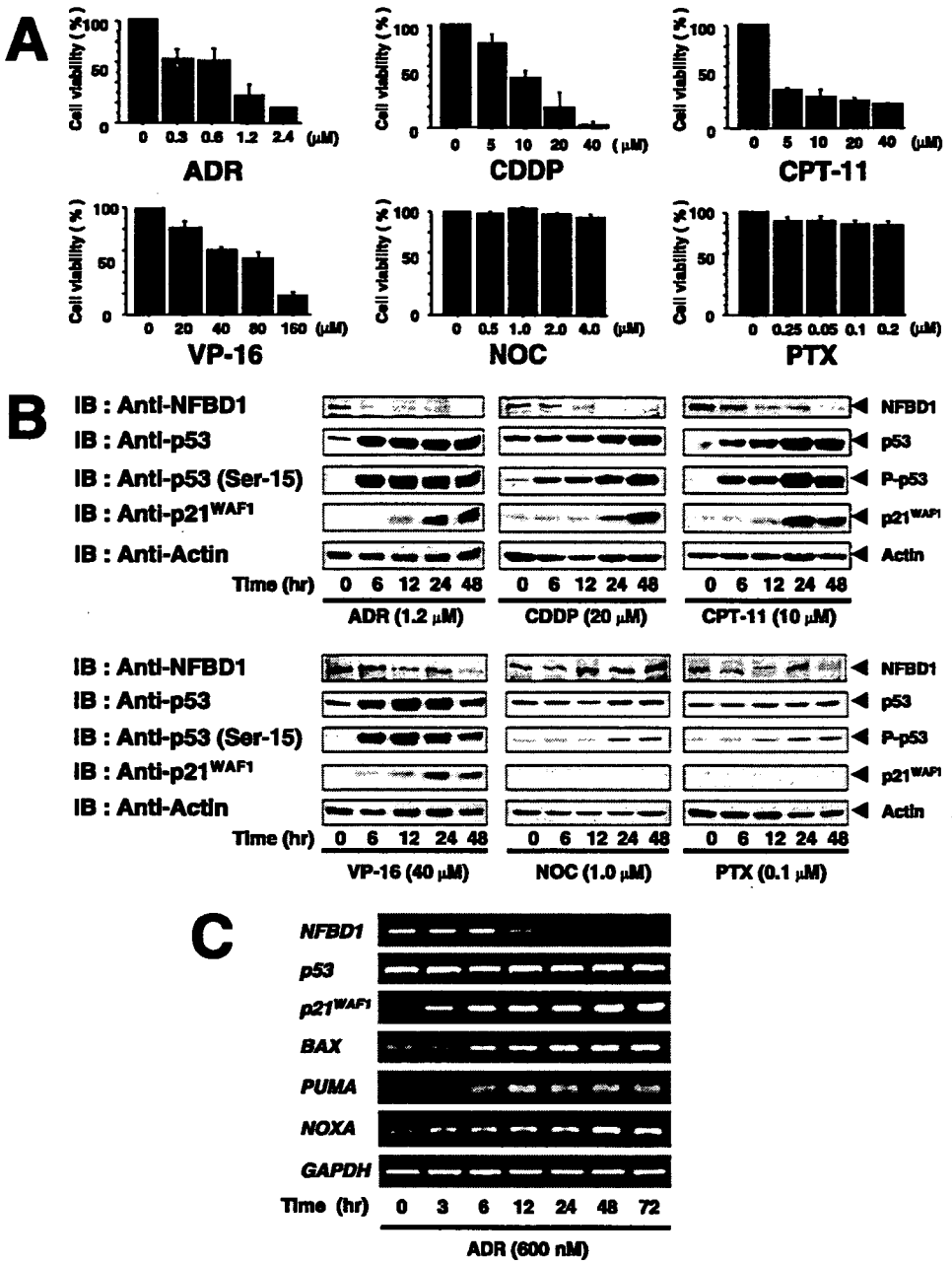

FIGURE 1. **Down-regulation of NFBD1 in association with the induction of p53 in response to genotoxic stresses.** *A*, cell survival assays. A549 cells were treated with various genotoxic agents, including ADR, CDDP, CPT-11, and VP-16 or with the nongenotoxic agents such as nocodazole (*NOC*) and PTX. Forty eight hours after treatment, cell viability was determined by MTT assays. Data are presented as the mean values ± S.D. of three independent experiments. *B*, down-regulation of NFBD1 following DNA damage. A549 cells bearing wild-type *p53* were exposed to ADR (1.2 μM), CDDP (20 μM), CPT-11 (10 μM), VP-16 (40 μM), nocodazole (1 μM), or PTX (0.1 μM). At the indicated time points after the drug treatment, whole cell lysates were prepared and analyzed by immunoblotting (*IB*) with the indicated antibodies. Immunoblotting for actin is shown as control for equal protein loading. *C*, RT-PCR analysis. A549 cells were treated with 600 nM ADR. At the indicated time periods after the treatment with ADR, total RNA was prepared and subjected to RT-PCR. *GAPDH* was used as an internal control.

Santa Cruz Biotechnology, Santa Cruz, CA), anti-actin (20–33; Sigma), anti-p53 (Ser-15) (16G8; Cell Signaling, Beverly, MA), or with anti-PUMA (Abcam, Cambridge, UK) antibody, followed by an incubation with horseradish peroxidase-conjugated goat anti-mouse or rabbit secondary antibody (Jackson ImmunoResearch, West Grove, PA). Protein-antibody complexes were visualized by enhanced chemiluminescence with the ECL system (Amersham Biosciences).

Immunoprecipitation—Precleared whole cell lysates were immunoprecipitated with normal rabbit serum (NRS) or with the anti-NFBD1 antibody, and the immunoprecipitates were recovered using protein G-Sepharose beads (Amersham Biosciences). After extensive washing with the lysis buffer, bound proteins were eluted out by boiling in SDS sample buffer and processed for immunoblotting with the indicated antibodies.

In Vitro Binding Assay—^{35}S-Labeled FLAG-tagged FHA, PST, and BRCT domains were transcribed and translated *in vitro* using the TnT T7 QuickCoupled transcription/translation system (Promega, Madison, WI). For pulldown assay, cell lysates prepared from COS7 cells were incubated with the radiolabeled proteins for 2 h at 4 °C. After incubation, the reaction mixture was immunoprecipitated with anti-p53 antibody (DO-1) for 2 h at 4 °C, followed by an incubation with protein G-Sepharose beads. The immunoprecipitates were recovered by brief centrifugation, washed with the lysis buffer, boiled in SDS sample buffer, and separated by 10% SDS-PAGE. After gel drying, radiolabeled proteins were visualized by autoradiography.

Indirect Immunofluorescence—For immunofluorescence, fixation was in 4% paraformaldehyde and permeabilization was in 0.2% Triton X-100. Coverslips were with anti-p53 (DO-1), anti-p53 (Ser-15) (16G8) or with anti-NFBD1 antibody. Cells were imaged by confocal microscope (Olympus, Tokyo, Japan).

Apoptosis Assay—A549 cells were transiently co-transfected with the constant amount of the expression plasmid for green fluorescence protein (GFP) together with or without the NFBD1 expression plasmid or the expression plasmid for siRNA against NFBD1. Twenty four hours after transfection, cells were treated with ADR or left untreated and incubated for another 24 h. Transfected cells were identified by the presence of green fluorescence. To verify apoptosis, cell nuclei were stained with DAPI to reveal nuclear condensation and frag-

mentation. The number of GFP-positive cells with apoptotic nuclei was scored.

Luciferase Reporter Assay—H1299 cells were transiently co-transfected with the indicated expression plasmids and reporter constructs. Forty eight hours post-transfection, whole cell lysates were prepared, and luciferase activity was assessed using a Promega dual luciferase assay system. The firefly luminescence signal was normalized based on the *Renilla* luminescence signal. The results were obtained from at least three sets of transfection and were presented as the mean ± S.D.

RESULTS

Down-regulation of NFBD1 in Response to a Variety of Genotoxic Agents—To explore the role of NFBD1 during the DNA damage response, we examined the expression kinetics of NFBD1 in human lung carcinoma A549 cells exposed to a variety of genotoxic agents, including ADR, camptothecin (CPT-11), cisplatin (CDDP), or etoposide (VP-16). In addition to the genotoxic agents, we also investigated the effect of nongenotoxic agents such as nocodazole (NOC) and paclitaxel (PTX) on NFBD1. A549 cells were exposed to the indicated agents at the concentrations recommended by Saito *et al.* (25). To examine the expression levels of NFBD1, we have generated a specific polyclonal antibody against the NH_2-terminal region of human NFBD1 (amino acid residues 1–150). The specificity of this antibody was verified by immunoblotting (data not shown). As shown in Fig. 1*A*, A549 cells treated with the indicated genotoxic agents underwent apoptosis in a dose-dependent manner as examined by MTT assay. Similar results were also obtained by fluorescence-activated cell sorter analysis (data not shown). In contrast, the nongenotoxic agents had undetectable effect on the viability of A549 cells. Immunoblot analysis revealed that the ADR treatment results in an accumulation of p53 as well as a phosphorylation of p53 at Ser-15, which is associated with a significant induction of one of the downstream effectors of p53, $p21^{WAF1}$ (Fig. 1*B*). It is worth noting that NFBD1 is strongly reduced in response to ADR in a time-dependent manner. Similar results were also obtained in A549 cells exposed to CPT-11, CDDP, or VP-16. On the other hand, NFBD1 levels remained unchanged even at the later time points after the addition of NOX or PTX. Additionally, the treatment of A549 cells with these nongenotoxic agents had a marginal effect on the accumulation of p53 and $p21^{WAF1}$ as compared with those of the genotoxic agents. Next, we performed RT-PCR using total RNA prepared from A549 cells exposed to 600 nM ADR for the indicated time periods. As shown in Fig. 1*C*, *NFBD1* mRNA levels were dramatically decreased in a time-dependent manner, accompanied with an up-regulation of *$p21^{WAF1}$*, *BAX*, *PUMA*, and *NOXA*. The expression levels of *p53* mRNA remained constant in ADR-treated A549 cells. These results suggest that NFBD1 is regulated at mRNA level in response to ADR.

Previously, it has been shown that NFBD1 associates with the members of the MRN complex, such as MRE11 and NBS1, and accumulates at nuclear foci in response to DNA damage (12, 14). Consistent with these observations, our immunofluorescence staining showed that NFBD1 co-localizes with NBS1 at nuclear foci within 1 h of exposing A549 cells to ADR, and NFBD1 nuclear foci are still present up to 24 h later (data not shown). ADR-mediated induction of p53 was undetectable after 1 h of treatment (Fig. 2*A*). Intriguingly, a significant nuclear accumulation as well as phosphorylation of p53 at Ser-15 was observed in cells 24 h after the treatment with ADR, which was associated with a disappearance of NFBD1 (Fig. 2, *A* and *B*). In contrast, NFBD1-containing nuclear foci were clearly present in cells lacking p53 induction. Collectively, these observations strongly suggest that there exists an inverse relationship between the expression of NFBD1 and p53 in response to DNA damage.

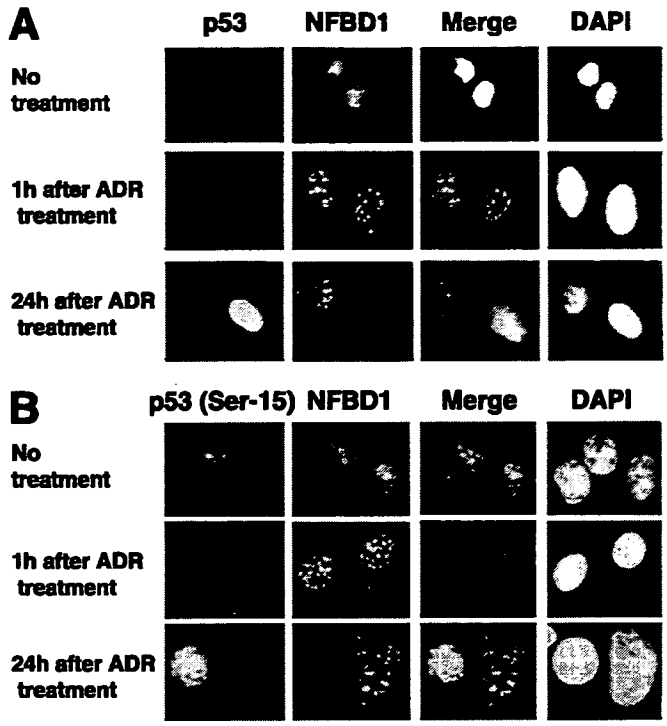

FIGURE 2. **Subnuclear localization of NFBD1 and p53 in response to ADR.** *A* and *B*, A549 cells were left untreated or treated with 600 nM ADR for the indicated time periods followed by incubation with the anti-NFBD1 and the anti-p53 antibodies (*A*), or with the anti-NFBD1 and anti-p53 (Ser-15) antibodies (*B*). Cell nuclei were stained with DAPI.

ADR-mediated Apoptosis in A549 Cells Is Regulated in a p53-dependent Manner—Because A549 cells carry wild-type *p53* (25), it is likely that the ADR-mediated apoptosis is regulated in a p53-dependent manner. To confirm this notion, we performed siRNA-mediated knockdown of p53. We transfected the empty plasmid or the expression plasmid for siRNA against p53 into A549 cells, and we established two control transfectants (C1 and C2) as well as two stable transfectants expressing siRNA for p53 (53R1 and 53R2) (Fig. 3*A*). We then performed MTT assay to examine a possible effect of p53 on the ADR-mediated apoptosis. As shown in Fig. 3*B*, 53R1 and 53R2 cells displayed a significant increase in cell viability as compared with the control transfectants and the parental A549 cells. Thus, it is likely that the ADR-mediated apoptosis in A549 cells is regulated at least in part in a p53-dependent manner.

To examine the possible effect of NFBD1 on the ADR-mediated apoptosis, A549 cells were transiently transfected with the empty plasmid or with the expression plasmid for NFBD1. Twenty four hours after transfection, cells were treated with

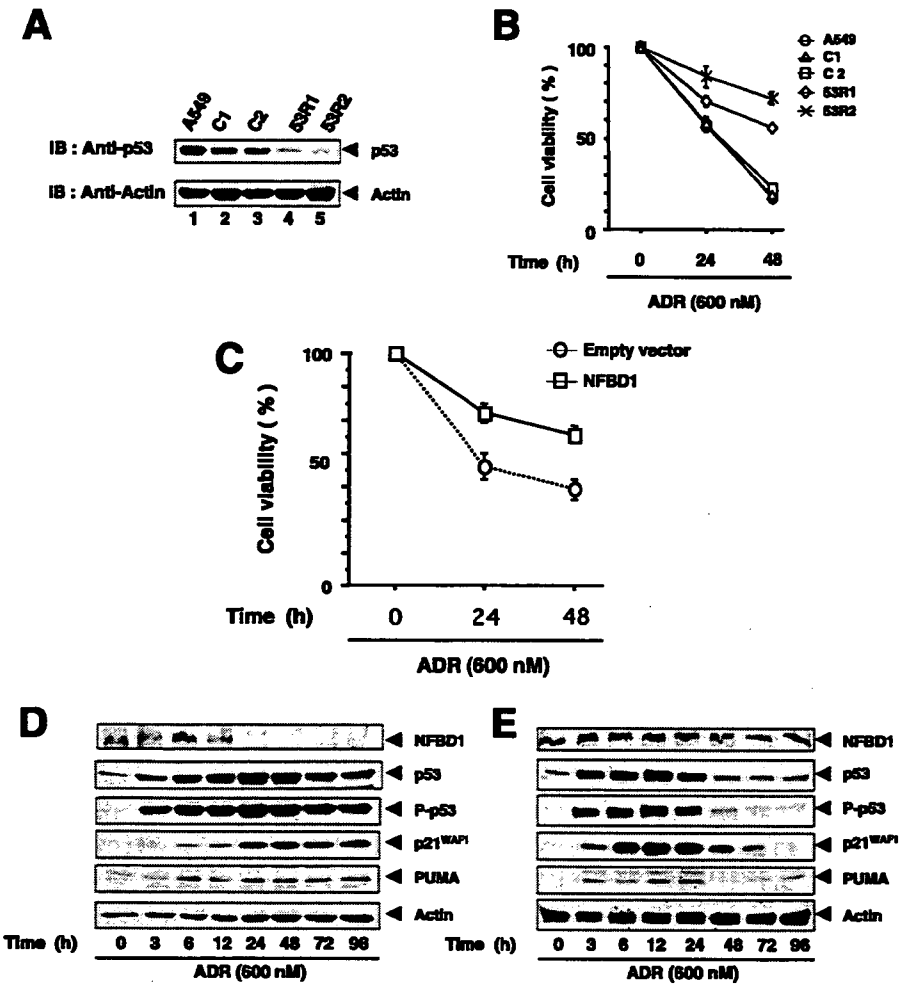

FIGURE 3. **ADR-mediated apoptosis in A549 cells is regulated in a p53-dependent manner.** *A*, knockdown of the endogenous p53. Whole cell lysates prepared from A549 cells stably expressing siRNA against p53 (53R1 and 53R2) or vector controls (*C1* and *C2*) were processed for immunoblotting (*IB*) with the anti-p53 antibody (*upper panel*). Whole cell lysates were also analyzed for actin as a control for protein loading and nonspecific RNA interference effects (*lower panel*). *B*, cell survival assay. Parental A549 (*open circle*), C1 (*open triangle*), C2 (*open square*), 53R1 (*open diamond*), and 53R2 cells (*cross*) were exposed to 600 nM ADR. At the indicated time periods after the treatment with ADR, their cell survivals were examined by MTT assay. *C*, cell survival assay. A549 cells were seeded in 6-well plates at a density of 1×10^5 cells/well and transiently transfected with 1 μg of the empty plasmid or with the NFBD1 expression plasmid. Twenty four hours after transfection, cells were exposed to 600 nM ADR. At the indicated time periods after the treatment with ADR, cell viability was examined by MTT assay. *D* and *E*, time course of the expression of p53 in response to ADR. A549 cells were transiently transfected with 2 μg of the empty plasmid (*D*) or with the expression plasmid for NFBD1 (*E*). Twenty four hours after transfection, cells were treated with 600 nM ADR. At the indicated time periods after the treatment with ADR, whole cell lysates were prepared and processed for immunoblotting with the indicated antibodies.

600 nM ADR. At the indicated time periods after the addition of ADR, cell viability was measured by MTT assay. As shown in Fig. 3*C*, the enforced expression of NFBD1 caused a remarkable increase in cell viability as compared with that of cells transfected with the empty plasmid. We next determined the time course of p53 expression in A549 cells overexpressing NFBD1 in response to ADR. As shown in Fig. 3*D*, ADR-mediated accumulation as well as phosphorylation of p53 at Ser-15 became detectable as early as 3 h of ADR exposure, and the levels of p53 were maintained up to 96 h in control cells. In addition, p53-dependent induction of $p21^{WAF1}$ and PUMA was detected at 6 h after the ADR treatment, and their expression levels persisted thereafter. In contrast, a significant reduction in the amounts and phosphorylation levels of p53 was detected in NFBD1-overexpressing cells at 24 h after the addition of ADR (Fig. 3*E*). This down-regulation of p53 was associated with a decrease in the expression levels of $p21^{WAF1}$ and PUMA. These results indicate that NFBD1 could inhibit the p53 phosphorylation at Ser-15, thereby reducing its transcriptional activity as well as stability.

NFBD1 Inhibits the p53-mediated Transcriptional Activation—To examine whether NFBD1 could affect the p53-mediated transcriptional activation, p53-deficient H1299 cells were transiently co-transfected with a constant amount of the expression plasmid for p53, luciferase reporter construct driven by the p53-responsive element derived from $p21^{WAF1}$, *MDM2*, or *BAX* promoter together with or without the increasing amounts of the NFBD1 expression plasmid, and luciferase activity was measured 48 h after transfection. As shown in Fig. 4, *A–C*, co-expression of p53 with NFBD1 resulted in a significant repression of the p53-mediated transcriptional activation. Consistent with the luciferase reporter assay, RT-PCR analysis revealed that NFBD1 inhibits the p53-mediated up-regulation of *PUMA* and *BAX* mRNA expression (Fig. 4*D*). To examine whether NFBD1 could affect the pro-apoptotic activity of p53, H1299 cells were transiently co-transfected with the indicated combinations of the expression plasmids, and their viability was measured by MTT assay. As shown in Fig. 4*E*, the enforced expression of p53 alone led to a decrease in cell viability as compared with that of cells transfected with the empty plasmid. As expected, p53-mediated decrease in cell viability was restored by co-expression with NFBD1.

Effect of NFBD1 on the ADR-mediated Apoptosis—Next, we sought to examine the possible effect of the endogenous NFBD1 on the ADR-mediated apoptosis. To this end, we utilized an siRNA-mediated knockdown of NFBD1 in A549 cells as shown in Fig. 5*A*. Silencing of NFBD1 in A549 cells resulted in an increased sensitivity to ADR as compared with the control cells (Fig. 5*B*). To confirm the anti-apoptotic effect of NFBD1 in detail, A549 cells were transiently co-transfected with the constant amount of the GFP expression plasmid together with the empty plasmid, or with the expression plasmid for NFBD1 or siRNA against NFBD1. GFP served as an indicator for transfected cells. Twenty four hours after transfection, cells were treated with 600 nM ADR or left untreated and incubated for

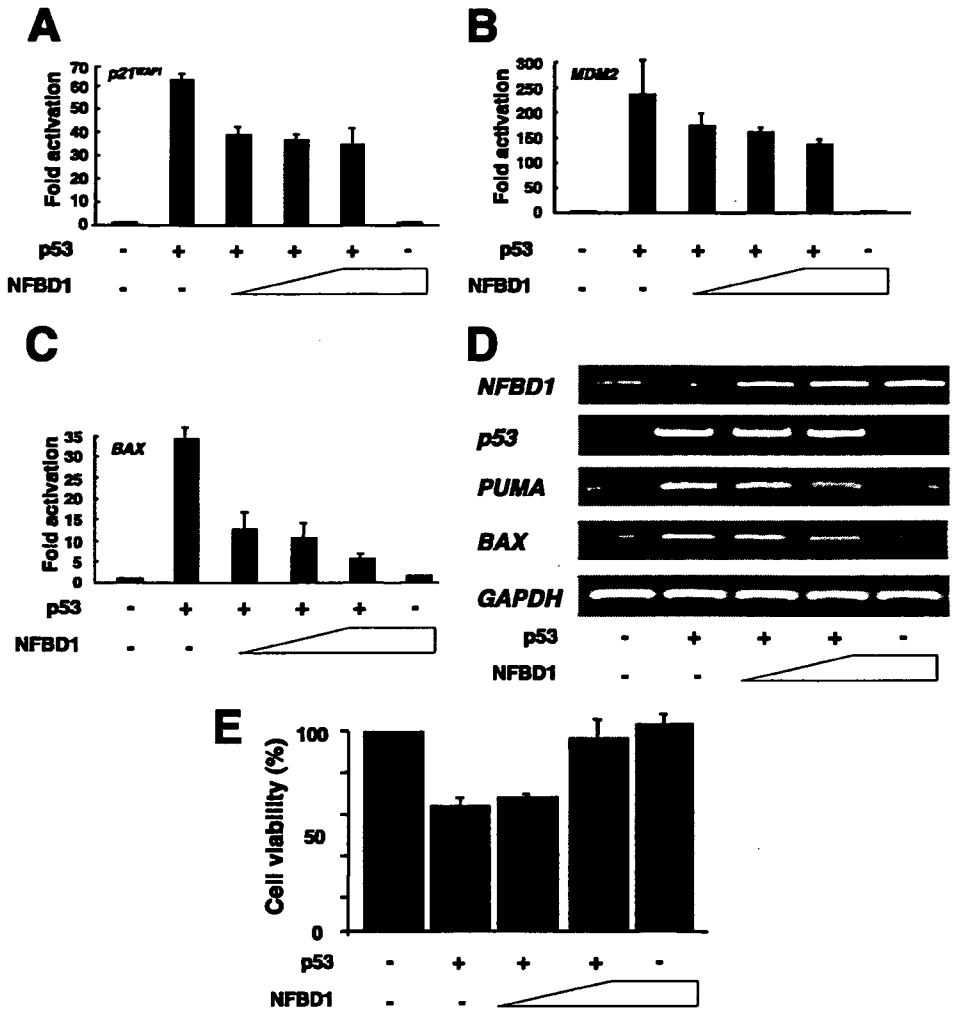

FIGURE 4. **NFBD1 inhibits the transcriptional activity as well as pro-apoptotic function of p53.** *A–C*, luciferase reporter analysis. H1299 cells were seeded in 12-well plates at a density of 5×10^4 cells/well. Cells were transiently co-transfected with 100 ng of the luciferase reporter construct carrying p53-responsive $p21_{WAF1}$ (*A*), *MDM2* (*B*), or *BAX* (*C*) promoter, 10 ng of pRL-TK *Renilla* luciferase cDNA, and 25 ng of the expression plasmid for p53 together with or without the increasing amounts of the NFBD1 expression plasmid (25, 50, and 100 ng). Following 48 h of incubation, luciferase activity was measured and normalized for transfection efficiency using *Renilla* luciferase activity. The results were obtained from at least three sets of transfection and were presented as the mean ± S.D. *D*, RT-PCR analysis. H1299 cells were transiently co-transfected with the constant amount of the expression plasmid for p53 (100 ng) together with or without the increasing amounts of the NFBD1 expression plasmid (400 and 800 ng). Twenty four hours after transfection, total RNA was prepared and analyzed by RT-PCR for the expression levels of *NFBD1*, *p53*, *PUMA*, and *BAX*. The expression level of *GAPDH* was measured as an internal control. *E*, cell survival assay. The constant amount of the p53 expression plasmid (200 ng) was transiently co-transfected into H1299 cells together with or without the increasing amounts of the NFBD1 expression plasmid (400 and 800 ng). Total amount of DNA was kept constant (1 μg) with the empty plasmid. Forty eight hours later, cell viability was examined by MTT assay.

another 24 h. Cell nuclei were then stained with DAPI, and the number of GFP-positive cells with apoptotic nuclei was scored. The enforced expression of NFBD1 led to a decrease in the number of apoptotic cells in response to ADR as compared with that of the control cells (Fig. 5, *C* and *D*). As expected, siRNA-mediated knockdown of NFBD1 caused a significant increase in the number of apoptotic cells in response to ADR. In contrast to A549 cells, overexpression of NFBD1 and silencing of NFBD1 in p53-deficient H1299 cells had an undetectable effect on the ADR-mediated apoptosis (Fig. 5*E*). Taken together, these results strongly suggest that NFBD1 prevents the ADR-mediated apoptosis by modulating p53.

Next, we examined the possible effect of the siRNA-mediated knockdown of the endogenous NFBD1 on the p53-mediated transcriptional activation. For this purpose, H1299 cells were transiently co-transfected with the constant amount of p53 expression plasmid together with or without the increasing amounts of the expression plasmid for siRNA against NFBD1. As shown in Fig. 6, *A–C*, siRNA-mediated knockdown of the endogenous NFBD1 in H1299 cells increased the p53-dependent luciferase activities driven from $p21^{WAF1}$, *MDM2*, or *BAX* promoter. In addition, similar results were obtained in U2OS cells bearing wild-type *p53* (supplemental Fig. 1). Furthermore, the down-regulation of the endogenous NFBD1 resulted in a significant increase in the phosphorylation levels of p53 at Ser-15 as well as the amount of p53 (Fig. 6*D*). Under our experimental conditions, the exogenously expressed p53 was phosphorylated in the absence of DNA-damaging agents. Similar observations were also described (26). These results strongly suggest that NFBD1 inhibits the transcriptional as well as pro-apoptotic activity of p53 through the down-regulation of p53.

Physical Interaction between NFBD1 and p53—To examine whether NFBD1 could interact with p53 in cells, whole cell lysates prepared from HEK293T cells were immunoprecipitated with NRS or with the polyclonal anti-NFBD1 antibody, and the immunoprecipitates were analyzed by immunoblotting with the monoclonal anti-p53 antibody. As shown Fig. 7*A*, the anti-NFBD1 immunoprecipitates contained the endogenous p53, suggesting that NFBD1 forms a complex with p53. Similarly, the anti-p53 immunoprecipitates contained the endogenous NFBD1. To map the region(s) of p53 required for the interaction with NFBD1, H1299 cells were transiently co-transfected with the expression plasmid for NFBD1 together with the expression plasmid for p53-(1–359), p53-(1–292), p53-(1–101), or with p53-(102–393) (Fig. 7*B*). Forty eight hours after transfection, whole cell lysates were prepared and processed for the immunoprecipitation with the indicated antibodies. As shown in Fig. 7, *C–F*, all of the p53 deletion mutants except p53-(102–393) retained an ability to interact with NFBD1,

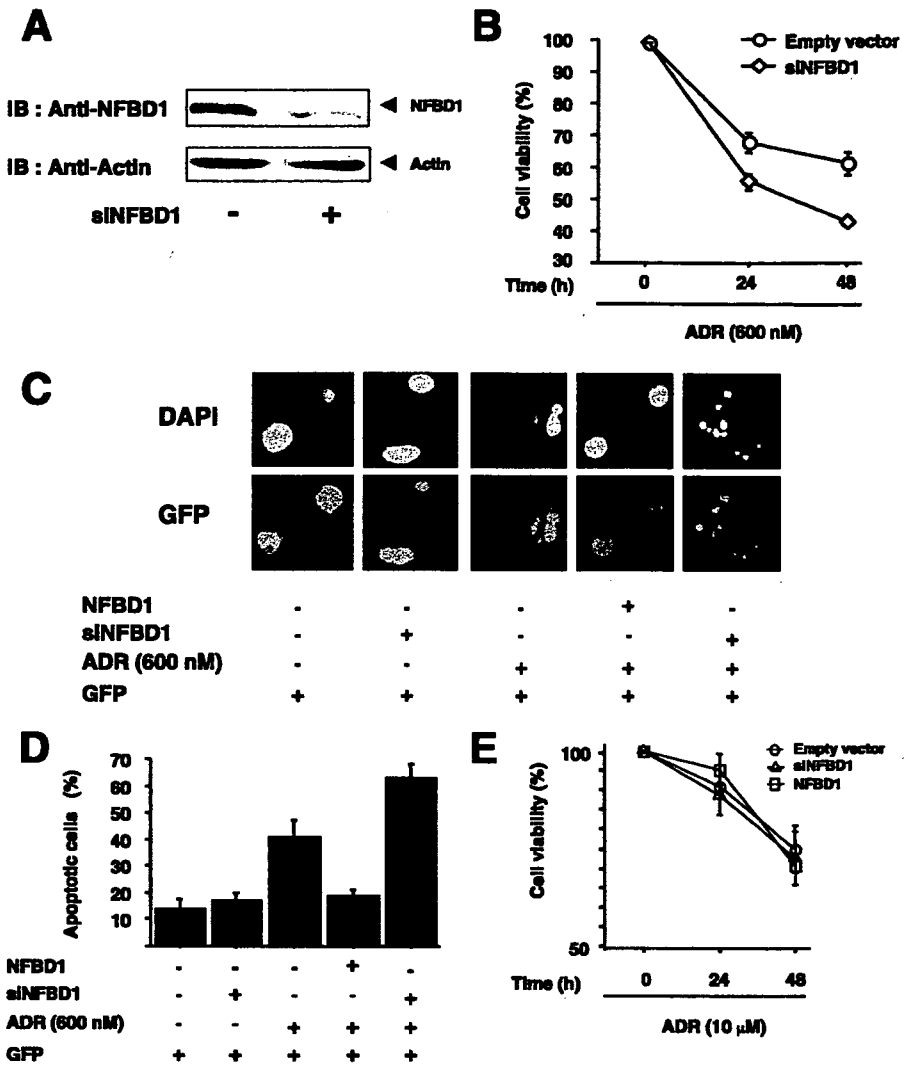

FIGURE 5. **siRNA-mediated down-regulation of the endogenous NFBD1 promotes the ADR-dependent apoptosis.** *A*, reduction of the endogenous NFBD1 by siRNA against NFBD1. A549 cells were transiently transfected with the expression plasmid for siRNA against NFBD1 termed siNFBD1or with the empty plasmid. Forty eight hours after transfection, whole cell lysates were analyzed for the expression level of the endogenous NFBD1 by immunoblotting (*IB*) and also analyzed for actin as a control for protein loading and nonspecific RNA interference effects. *B*, cell survival assay. A549 cells were transiently transfected with the empty plasmid (*open circle*) or with NFBD1-siRNA (*open diamond*). Twenty four hours post-transfection, cells were treated with 600 nM ADR. At the indicated time periods after the treatment with ADR, cell viability was measured by MTT assay. *C* and *D*, apoptosis assay. A549 cells were transiently co-transfected with the constant amount of the expression plasmid for GFP together with or without the NFBD1 expression plasmid or siNFBD1. Twenty four hours after transfection, cells were treated with ADR (600 nM) for another 24 h. Cell nuclei were stained with DAPI, and transfected cells were identified by the presence of green fluorescence (*C*). The number of GFP-positive cells with apoptotic nuclei was scored (*D*). *E*, NFBD1 has undetectable effect on the ADR-induced apoptosis in p53-deficient H1299 cells. H1299 cells were transfected with the empty plasmid (*open circle*), expression plasmid for NFBD1 (*open square*), or siNFBD1 (*open triangle*). Twenty four hours after transfection, cells were exposed to 10 μM ADR for 24, 48, and 72 h, and their viability was then examined as described in *B*.

suggesting that the NH_2-terminal region of p53 is required for the interaction with NFBD1.

Phosphorylated Forms of p53 Do Not Bind to NFBD1—Our preliminary experiments indicated that λ-phosphatase treatment of ADR-treated whole cell lysates significantly increases an ability of BRCT domain of NFBD1(see below) to interact with endogenous p53 (data not shown). These results prompted us to examine whether the phosphorylation of p53 could affect the interaction with NFBD1. As shown in Fig. 8, the detailed analysis of the time course of NFBD1/p53 interaction in A549 cells in response to ADR demonstrated that p53 phosphorylated at Ser-15 fails to be co-immunoprecipitated with NFBD1 during the ADR-mediated apoptosis. In addition, the NFBD1-p53 complex was detected in untreated cells and remained at high levels for 3 h of the ADR treatment, after which the amounts of this complex slowly decreased.

BRCT Domain of NFBD1 Is Required for the Interaction with p53—We sought to determine the essential region(s) of NFBD1 required for the interaction with p53. To this end, we generated the expression plasmids for FLAG-FHA, FLAG-PST, and FLAG-BRCT (Fig. 9*A*). To examine the subcellular distribution of the NFBD1 deletion mutants, COS7 cells were transiently transfected with these expression plasmids. Forty eight hours after transfection, cells were fractionated into nuclear and cytoplasmic fractions and subjected to immunoblotting. As shown in Fig. 9*B*, FLAG-PST and FLAG-BRCT were expressed in both the nucleus and cytoplasm, whereas FLAG-FHA was detected in the cytoplasm. Because of the different subcellular distribution of the NFBD1 deletion mutants, we performed the *in vitro* pulldown assays. Whole cell lysates prepared from COS7 cells were incubated with the radiolabeled NFBD1 deletion mutants and then immunoprecipitated with the anti-p53 antibody. The anti-p53 immunoprecipitates were analyzed by SDS-PAGE followed by autoradiography. As shown in Fig. 9*C*, the BRCT domains were required for the maximal binding to p53.

The BRCT Domains of NFBD1 Have an Ability to Down-regulate p53—To investigate the functional significance of the BRCT domains of NFBD1 in the regulation of p53, A549 cells were transiently transfected with or without the increasing amounts of the expression plasmid for FLAG-BRCT. Twenty four hours after transfection, cells were exposed to ADR and incubated for another 24 h. Whole cell lysates were then prepared and subjected to immunoblotting with the indicated antibodies. FLAG-FHA was used as a negative control. As shown in Fig. 10*A*, the ADR-mediated accumulation and phosphorylation of p53 at Ser-15 were inhibited by FLAG-BRCT. This down-regulation of p53 was associated with a decrease in the expression levels of BAX and $p21^{WAF1}$. In contrast, FLAG-

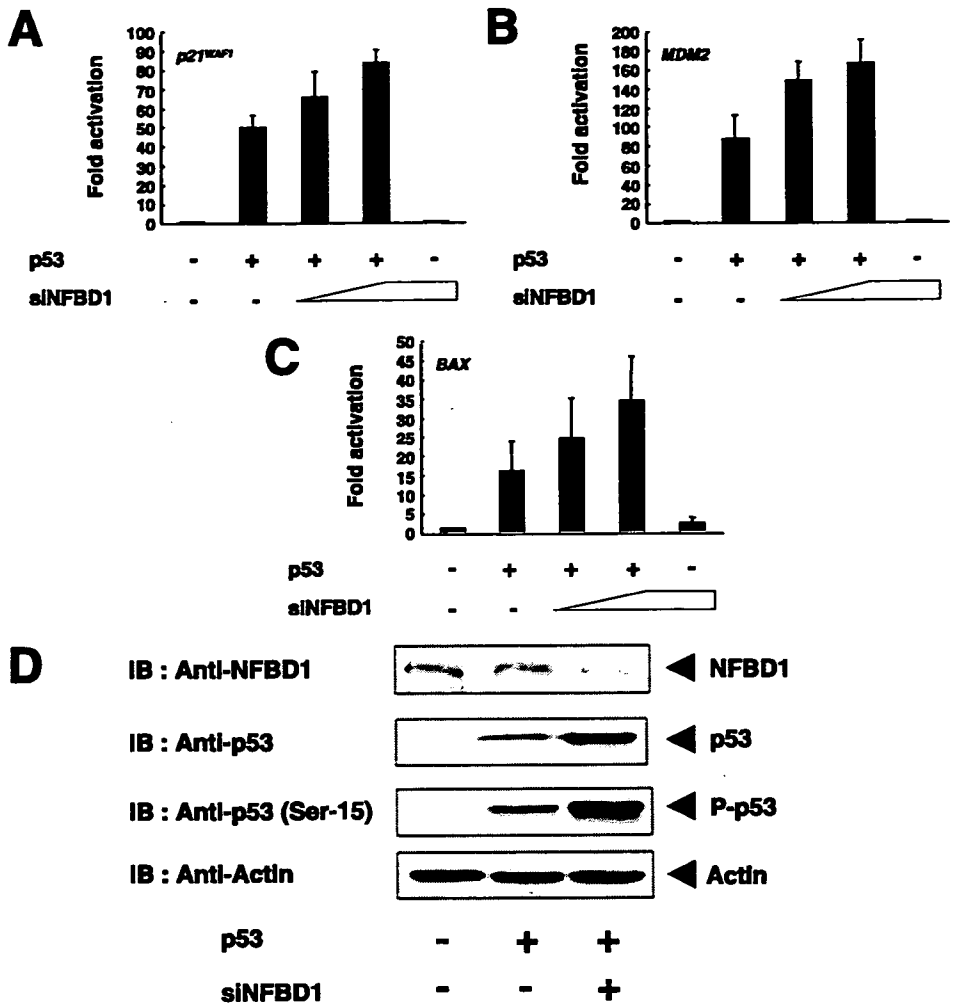

FIGURE 6. **siRNA-mediated knockdown of NFBD1 enhances the p53-dependent transcriptional activation.** *A–C*, luciferase reporter analysis. H1299 cells were transiently co-transfected with the constant amount of the expression plasmid for p53, luciferase reporter construct driven by the p53-responsive element derived from $p21^{WAF1}$ (*A*), *MDM2* (*B*), or *BAX* (*C*) promoter, and pRL-TK *Renilla* luciferase cDNA together with or without the increasing amounts of the expression plasmid for siRNA against NFBD1. Forty eight hours after transfection, cell lysates were prepared, and luciferase activity was measured. *D*, siRNA-mediated knockdown of NFBD1 increases the phosphorylation of p53 at Ser-15. H1299 cells were transiently co-transfected with the constant amount of the expression plasmid for p53 together with or without the expression plasmid encoding siRNA against NFBD1. Whole cell lysates were examined by immunoblotting (*IB*) with the indicated antibodies.

FHA, which was localized exclusively in cytoplasm, had no significant effect on p53 (Fig. 10*B*). Thus, it is likely that the BRCT domains of NFBD1 play a crucial role not only in the physical interaction with p53 but also in the down-regulation of p53.

DISCUSSION

A growing body of evidence strongly suggests that NFBD1 mediates the rapid recruitment of the MRN complex into the sites of DNA damage, and thus facilitates the efficient repair of DNA double strand breaks before the cells undergo DNA replication (27). NFBD1 also has an anti-apoptotic function in response to DNA damage. For example, siRNA-mediated depletion of the endogenous NFBD1 resulted in the increased sensitivity to irradiation and anti-cancer drug (13–16). Recently, it has been shown that NFBD1-deficient mice display the abnormal phenotypes, including chromosome instability, DNA repair defects, and radiation sensitivity (28). However, the detailed molecular mechanism behind the anti-apoptotic effect of NFBD1 is still largely elusive. In this study, we have found that NFBD1 interacts with tumor suppressor p53, reduces its phosphorylation at Ser-15 in response to ADR, and thereby inhibiting the transcriptional as well as pro-apoptotic activity of p53. Thus, our present findings would help to shed light on the currently unknown molecular mechanisms underlying the NFBD1-mediated anti-apoptotic effect in response to DNA damage.

During the DNA damage-induced apoptosis, p53 is activated by a complex series of phosphorylations within its NH_2-terminal transactivation domain (reviewed in Ref. 24). The catalytic activity of ATM is markedly increased in response to DNA damage and is responsible for the rapid phosphorylation of p53 at Ser-15, as described previously (20, 21). This ATM-mediated phosphorylation contributes to the enhanced activity as well as stability of p53 by facilitating its dissociation from E3 ubiquitin protein ligase MDM2 (29). When Ser-15 was replaced by Ala, the transcriptional activity of p53 was significantly reduced (30). Under our experimental conditions, ADR treatment induced p53 accumulation and phosphorylation at Ser-15 in A549 cells. Recently, Peng and Chen (31) reported that 53BP1 and NFBD1 are required for the recruitment of ATM-Rad3-related into the DNA damage sites, suggesting that ATM-Rad3-related as well as ATM might also participate in this process. On the other hand, little increase in phosphorylation at Ser-20 as well as Ser-46 in response to ADR was observed at any time examined (data not shown). It is worth noting that the ADR-induced phosphorylation of p53 at Ser-15 was associated with a strong down-regulation of NFBD1, and the high p53 phosphorylation levels persisted even 96 h after the treatment. Constitutive expression of NFBD1 resulted in a remarkable decrease in the phosphorylation levels of p53 at Ser-15 24–48 h after the ADR treatment. Consistent with these results, the siRNA-mediated knockdown of the endogenous NFBD1 in H1299 cells led to a significant phosphorylation of the exogenous p53 at Ser-15, indicating that NFBD1 has an inhibitory role in the regulation of p53. This notion was further supported by the facts that the p53-mediated transcriptional activation and apoptosis are impaired by NFBD1.

Based on our immunoprecipitation experiments, NFBD1 bound to the NH_2-terminal region of p53, including its transactivation domain. MDM2 attenuates the transcriptional activity of p53 by binding to and masking its transactivation domain, as described previously (32). MDM2 also acts as an E3 ubiquitin protein ligase for p53 and promotes its ubiquitination-dependent proteasomal turnover. It has been shown that Ser-15 phosphorylation impairs the interaction between p53 and MDM2 and leads to the subsequent stabilization and activation of p53 (29). Phosphorylation at Ser-15 also stimulates p53 interaction with its transcriptional co-activators such as p300/CBP (30, 33). Alternatively, tumor suppressor $p19^{ARF}$ directly interacts with MDM2 to inhibit its E3 ubiquitin protein ligase activity, thereby preventing the MDM2-mediated degradation of p53 (34–37). In addition, Maya *et al.* (38) reported that MDM2 is phosphorylated by ATM in response to DNA damage, and this phosphorylation attenuates its inhibitory potential on p53. Our preliminary results indicated that NFBD1 is associated with MDM2 as examined by co-immunoprecipitation assay (data not shown). Considering that NFBD1 directly interacts with the NH_2-terminal region of p53, it is likely that NFBD1 might mask the Ser-15 to prevent its phosphorylation mediated by ATM, and/or recruit MDM2 to the NH_2-terminal region of p53 to facilitate MDM2-mediated proteolytic degradation of p53. Further studies will be necessary to clarify this issue.

NFBD1 contains several protein-protein interaction domains. Xu and Stern (15) demonstrated that NFBD1-derived FHA and BRCT domains are necessary for the interaction with MRN complex and γH2AX, respectively. According to our *in vitro* binding analysis, NFBD1 bound to p53 mainly through its BRCT domains. Consistent with these results, BRCT domains of NFBD1 retained an abil-

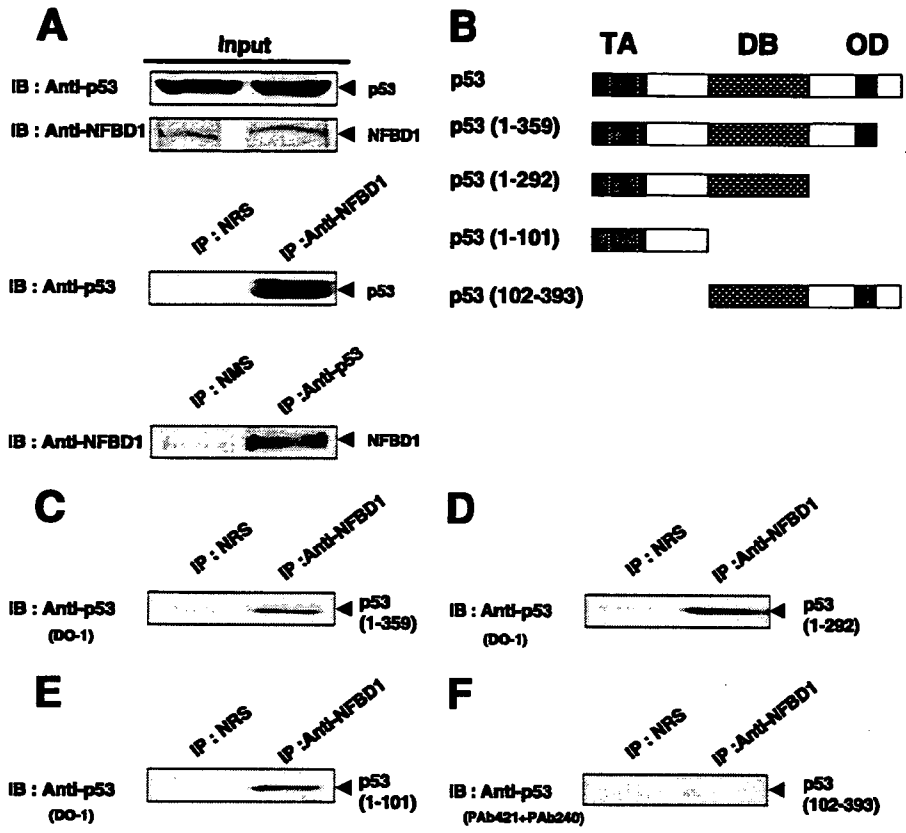

FIGURE 7. **Interaction between NFBD1 and p53 in cells.** *A*, immunoprecipitation. Whole cell lysates prepared from HEK293T cells were immunoprecipitated (*IP*) with NRS or with the polyclonal anti-NFBD1 antibody, or immunoprecipitated with normal mouse serum (*NMS*) or with monoclonal anti-p53 antibody, and the immunoprecipitates were analyzed by immunoblotting (*IB*) with the monoclonal anti-p53 or with polyclonal anti-NFBD1 antibody, respectively. *B*, schematic drawing of the full-length p53 and various p53 deletion mutants used in this study. *TA*, transactivation domain; *DB*, DNA-binding domain; *OD*, oligomerization domain. *C–F*, NFBD1 interacts with the NH_2-terminal region of p53 containing its transactivation domain. H1299 cells were transiently co-transfected with the indicated combinations of the expression plasmids. Forty eight hours after transfection, whole cell lysates were prepared and subjected to immunoprecipitation with NRS or with the polyclonal anti-NFBD1 antibody followed by immunoblotting with the indicated anti-p53 antibodies.

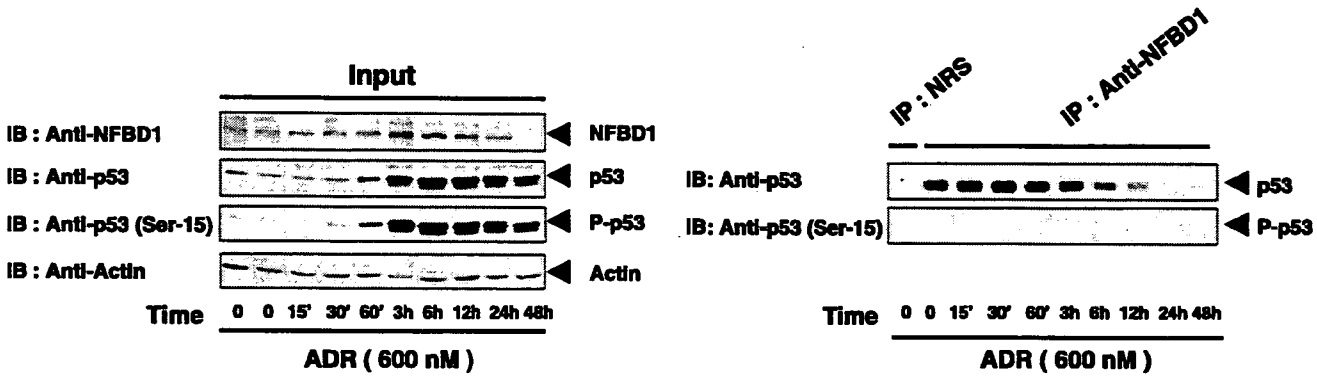

FIGURE 8. **p53 phosphorylated at Ser-15 does not interact with NFBD1 in cells.** A549 cells were exposed to 600 nM ADR. At the indicated time points after the treatment with ADR, whole cell lysates were prepared and immunoprecipitated (*IP*) with NRS or with the anti-NFBD1 antibody followed by immunoblotting (*IB*) with the anti-p53 or with the anti-p53 (Ser-15) antibody (*right panel*). Input amounts of proteins were determined by immunoblotting with the indicated antibodies (*left panel*). Actin was used as a loading control.

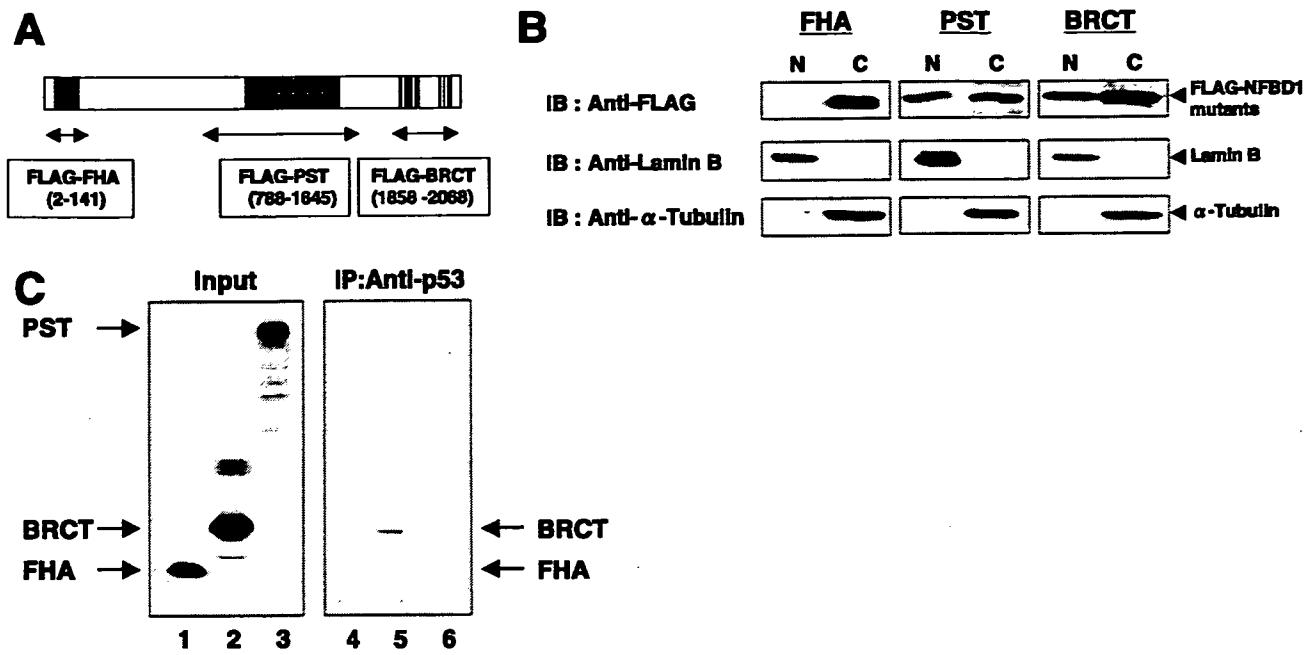

FIGURE 9. **BRCT domains of NFBD1 are required for the interaction with p53.** *A*, schematic representation of FLAG-NFBD1 mutants. *Number* indicates amino acid position. *B*, subcellular localization of NFBD1 mutants. COS7 cells were transiently transfected with the indicated expression plasmids. Forty eight hours after transfection, cells were fractionated into nuclear (*N*) and cytoplasmic (*C*) fractions. Equal amounts of each fraction were separated by 10% SDS-PAGE and immunoblotted (*IB*) with the anti-FLAG antibody (*top panel*). Samples were also immunoblotted with the antibody specific for lamin B (*middle panel*) or with the anti-α-tubulin (*bottom panel*) to show the purity of each fraction. *C*, *in vitro* binding assay. Whole cell lysates prepared from COS7 cells were incubated with the radiolabeled FLAG-FHA, FLAG-BRCT, or with FLAG-PST and immunoprecipitated (*IP*) with the anti-p53 antibody. Immunoprecipitates were separated by 10% SDS-PAGE, and the radiolabeled bound proteins were visualized by autoradiography.

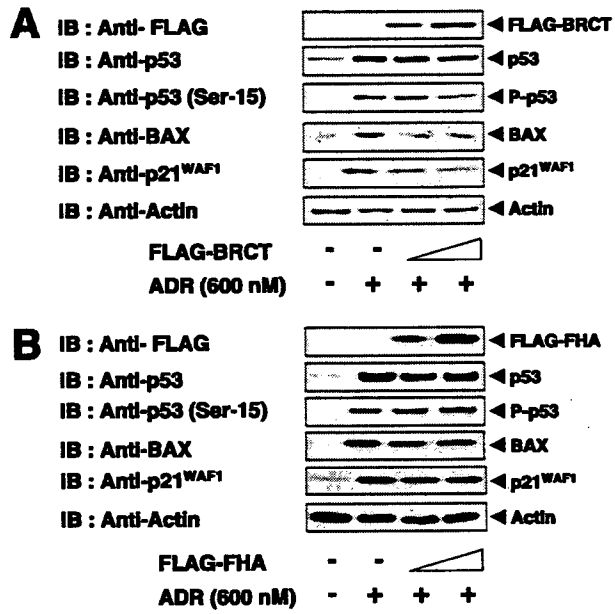

FIGURE 10. **BRCT domains of NFBD1 retain an ability to inhibit the induction of p53 in response to ADR.** *A* and *B*, immunoblot (*IB*) analysis. A549 cells were transiently transfected with the increasing amounts of the FLAG-BRCT (*A*) or with the FLAG-FHA expression plasmid (*B*). The total amount of DNA was kept constant (2 μg) with pcDNA3. Twenty four hours after transfection, cells were left untreated or treated with 600 nM ADR and incubated for another 24 h. Whole cell lysates were then prepared and analyzed by immunoblotting with the indicated antibodies.

ity to reduce the p53 phosphorylation levels at Ser-15 as well as to decrease the stability of p53. In contrast, the FHA domain-containing fragment had no significant effect on p53 because of its cytoplasmic localization. BRCT domains mediate phosphorylation-dependent protein-protein interaction, as described previously (39–41). For example, the BRCT domains of BRCA1 recognize specific phospho-Ser-containing peptides (40). In contrast, unphosphorylated forms of p53 bound to the BRCT domains of NFBD1 much more efficiently *in vitro* relative to phosphorylated forms of p53 (data not shown). Furthermore, NFBD1 failed to bring down p53 phosphorylated at Ser-15 as examined by co-immunoprecipitation experiments. Thus, it is likely that BRCT domains of NFBD1 do not always prefer phospho-Ser-containing peptides.

It has been shown that NFBD1 cooperates with the histone variant H2AX to recruit DNA repair proteins such as MRN complex to the sites of DNA damage (27). In accordance with this notion, NFBD1 displayed diffuse nuclear staining under normal conditions, whereas NFBD1 redistributed to nuclear foci within 1 h after the treatment with ADR. The NFBD1 nuclear foci co-localized with NBS1 and lasted at least 24 h after the ADR treatment (data not shown). The ADR-induced accumulation of p53 was not clearly detected within 1 h of exposure. At a single cell level, the ADR-induced NFBD1 nuclear foci were present only in cells lacking p53 accumulation and phosphorylation at Ser-15 24 h after the treatment. In contrast, NFBD1 nuclear foci were undetectable in cells expressing p53. These observations were consistent with the inverse relationship between the expression levels of p53 and NFBD1 in response to ADR. Considering that NFBD1 directly interacts with p53, thereby preventing its phosphorylation at Ser-15, it is possible that NFBD1 participates in the early cellular responses to ADR, and the ADR-induced down-regulation of NFBD1 might be crucial for the initiation of the p53-dependent apoptotic response.